AD-A035 891 NAVAL POSTGRADUATE SCHOOL MONTEREY CALIF F/G 4/2
STUDY OF MONSOON CIRCULATION WITH STEADY AND FLUCTUATION HEATIN--ETC(U)
DEC 76 R J PENTIMONTI

UNCLASSIFIED NL

1 OF 1
AD
A035891

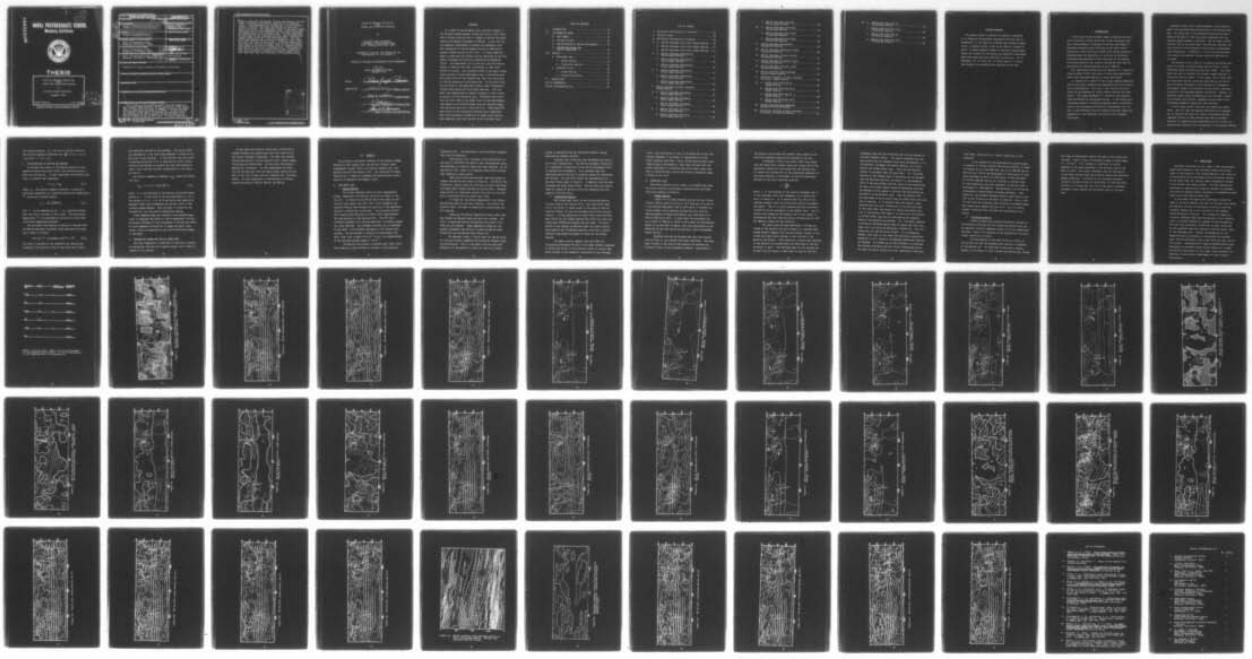

END

DATE
FILMED
3-77

NAVAL POSTGRADUATE SCHOOL
Monterey, California

THESIS

STUDY OF MONSOON CIRCULATION
WITH
STEADY AND FLUCTUATING HEATING

by

Richard Joseph Pentimonti

December 1976

Thesis Advisor: C.-P. Chang

SECURITY CLASSIFICATION OF THIS PAGE (When Data Entered)

REPORT DOCUMENTATION PAGE

READ INSTRUCTIONS BEFORE COMPLETING FORM

1. REPORT NUMBER

2. GOVT ACCESSION NO.

3. RECIPIENT'S CATALOG NUMBER

4. TITLE (and Subtitle)

Study of Monsoon Circulation with Steady and Fluctuating Heating.

5. TYPE OF REPORT & PERIOD COVERED

Master's Thesis; December 1976

6. PERFORMING ORG. REPORT NUMBER

7. AUTHOR(s)

Richard Joseph Pentimonti

8. CONTRACT OR GRANT NUMBER(s)

9. PERFORMING ORGANIZATION NAME AND ADDRESS

Naval Postgraduate School
Monterey, California 93940

10. PROGRAM ELEMENT, PROJECT, TASK AREA & WORK UNIT NUMBERS

11. CONTROLLING OFFICE NAME AND ADDRESS

Naval Postgraduate School
Monterey, California 93940

12. REPORT DATE

December 1976

13. NUMBER OF PAGES

68

14. MONITORING AGENCY NAME & ADDRESS(if different from Controlling Office)

Naval Postgraduate School
Monterey, California 93940

67p.

15. SECURITY CLASS. (of this report)

Unclassified

15a. DECLASSIFICATION/DOWNGRADING SCHEDULE

16. DISTRIBUTION STATEMENT (of this Report)

Approved for public release; distribution unlimited.

17. DISTRIBUTION STATEMENT (of the abstract entered in Block 20, if different from Report)

18. SUPPLEMENTARY NOTES

19. KEY WORDS (Continue on reverse side if necessary and identify by block number)

20. ABSTRACT (Continue on reverse side if necessary and identify by block number)

In a study of the planetary-scale vorticity budget of the northern summer monsoon, Holton and Colton (1972) found that a strong vorticity sink is needed to balance the generation by horizontal divergence at 200 mb. In this work we use numerical experiments to examine the hypothesis that the fluctuation of the divergence forcing as observed by several studies serves as this sink. A 3-level numerical

Next Page

DD FORM 1 JAN 73 1473 (Page 1)

EDITION OF 1 NOV 65 IS OBSOLETE
S/N 0102-014-6601

SECURITY CLASSIFICATION OF THIS PAGE (When Data Entered)

251 450

model is used with the thermal forcing specified by the horizontal divergence distribution observed by Krishnamurti (1971). Two experiments are carried out, one with heating steady in time and the other fluctuating in time with a period of 10 days. The time-mean fields of the quasi-steady state solution in both experiments show a significant westward phase shift of the Tibetan high, thus the fluctuation of heating cannot be a sufficient sink. On the other hand, the positions of the simulated tropical upper tropospheric troughs agree quite well with those observed. This suggests that damping due to cumulus transport is more likely to account for the vorticity sink. Transient wave activities are also found at the upper level in both experiments. They appear to be drawing energy from the planetary-scale flow and could serve as a vorticity sink. These waves are most active in the fluctuating heating case, suggesting that local barotropic instability at upper levels may be more important than that implied by the time-mean wind.

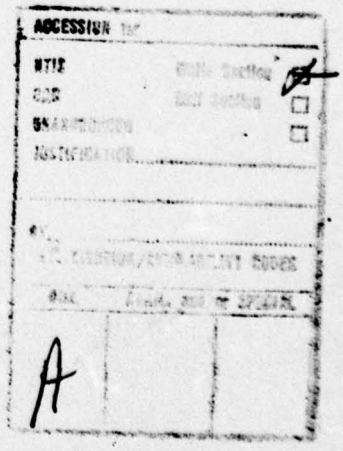

Study of Monsoon Circulation with Steady and Fluctuating Heating

by

Richard Joseph Pentimonti
Lieutenant, United States Navy
B.S., Gonzaga University, 1967

Submitted in partial fulfillment of the requirements for the degree of

MASTER OF SCIENCE IN METEOROLOGY AND OCEANOGRAPHY

from the

NAVAL POSTGRADUATE SCHOOL
December 1976

Author 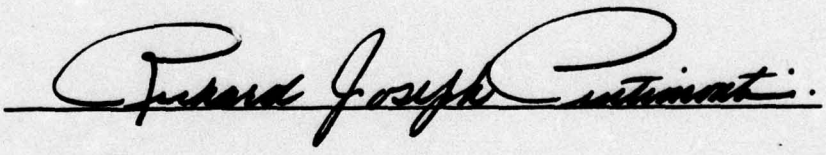

Approved by: 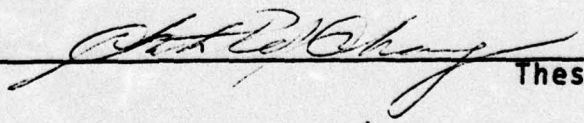
Thesis Advisor

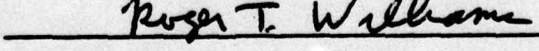
Second Reader

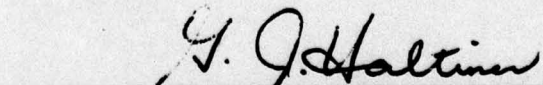
Chairman, Department of Meteorology

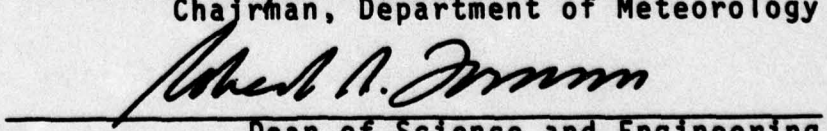
Dean of Science and Engineering

ABSTRACT

In a study of the planetary-scale vorticity budget of the northern summer monsoon, Holton and Colton (1972) found that a strong vorticity sink is needed to balance the generation by horizontal divergence at 200 mb. In this work we use numerical experiments to examine the hypothesis that the fluctuation of the divergence forcing as observed by several studies serves as this sink. A 3-level numerical model is used with the thermal forcing specified by the horizontal divergence distribution observed by Krishnamurti (1971). Two experiments are carried out, one with heating steady in time and the other fluctuating in time with a period of 10 days. The time-mean fields of the quasi-steady state solution in both experiments show a significant westward phase shift of the Tibetan high, thus the fluctuation of heating cannot be a sufficient sink. On the other hand, the positions of the simulated tropical upper tropospheric troughs agree quite well with those observed. This suggests that damping due to cumulus transport is more likely to account for the vorticity sink. Transient wave activities are also found at the upper level in both experiments. They appear to be drawing energy from the planetary-scale flow and could serve as a vorticity sink. These waves are most active in the fluctuating heating case, suggesting that local barotropic instability at upper levels may be more important than that implied by the time-mean wind.

TABLE OF CONTENTS

LIST OF FIGURES

ACKNOWLEDGEMENTS

The author wishes to express his thanks to Professor C.-P. Chang for his guidance throughout this work and to Professor R. T. Williams for offering many valuable suggestions. A special thanks is due to Mr. David F. Norman of the W. R. Church Computer Center of the Naval Postgraduate School for without his assistance the numerical experiments would have been much more difficult to carry out. Mr. M. McDermett, Mr. R. Alvis, Mr. A. Tellez and Mr. S. Rinard have helped in the handling and drafting of the data.

I. INTRODUCTION

In the study of the northern summer planetary-scale monsoon circulation, Holton and Colton (1972) discovered that very strong damping is necessary to balance the budget of time-mean planetary-scale vorticity at the upper levels. Specifically they found that without this strong damping to counterbalance the generation of vorticity by horizontal divergence the amplitude of the long waves of the monsoon circulation would be too large at the 200 mb level and the phase would be shifted westward by up to 5000 km.

This same phase problem was also apparent in a numerical study by Abbot (1971), who used a 2 layer quasi-geostrophic model with prescribed heating to study the monsoon.

In looking for a source of this strong damping mechanism, Holton and Colton suggested two hypotheses which may explain this strong damping. The first is the vertical mixing of vorticity and momentum by strong cumulus updrafts and downdrafts. The second hypothesis is related to the observed time fluctuation of the monsoon system. If the large-scale divergence contains a strong fluctuation then a correlation term of the divergence and vorticity fluctuations will appear in the time-mean vorticity equation and may reduce the generation of the time-mean vorticity by the time-mean divergence.

Murakami (1974) used a three-component, quasi-spectral model with prescribed heating which has a fluctuating component. He found that it can reasonably simulate the amplitude and the phase of the long waves associated with the northern summer monsoon circulation. But his model suffers from the lack of the zonal basic flow and the resultant vertical profile of the divergence field differs considerably from observations. Therefore it is not clear which mechanism causes the seemingly correct phase and amplitude of his model.

The purpose of this study is to examine the second hypothesis of Holton and Colton using the non-linear, finite difference model of Monaco and Williams (1975). This same model was used to simulate the northern summer monsoon circulation by Bellis (1975). In his study, Bellis found that the prescribed heating, which was specified by the 200 mb mean horizontal divergence field observed by Krishnamurti and Rodgers (1970), can reasonably excite several important features of the time-mean monsoon circulation. However, if extremely large values of damping are not included, a phase shift problem still exists, although the amplitude of the disturbance seemed to agree with that observed.

In this study we will carry out two controlled experiments. One will have the heating specified to be independent of time and the other will have a fluctuating heating component similar to that observed and used by Murakami. Hopefully by comparing these experiments we will be able to evaluate the effects of this fluctuation in the monsoon heating.

Another purpose of this study is to simulate the barotropic instability of the tropical easterly jet associated with the northern summer monsoon. This instability arises as a result of the strong easterly jet in the upper troposphere and has been studied by Colton (1974) and Bellis (1975). It represents an important scale-interaction mechanism for the monsoon circulation, according to the observational study by Krishnamurti (1971).

II. THE NUMERICAL MODEL

A. BASIC MODEL

The numerical model used was formulated by Monaco and Williams (1975) and is similar to that described by Arakawa and Mintz (1974) who used the primitive equations in spherical coordinates with "sigma" as the vertical coordinate. In this study the domain of calculation is restricted to the band between 18°S and 46°N for the sake of computer economy, and a free slip condition is applied at the lateral boundaries. The model has been previously used by Bellis (1975) for the area of 0°E to 180°E only.

B. THE GRID SYSTEM

The horizontal distribution of variables is illustrated in Figure 1 which is the so-called C-scheme arrangement (Arakawa and Mintz, 1974). The grid spacing is 4 degrees in both latitude and longitude. The troposphere is divided into seven equally spaced sigma layers in the vertical with three main reporting levels, as shown in Figure 2. The sigma coordinate is defined as

$$\sigma \equiv \frac{p - p_t}{\pi} \tag{2.1}$$

where p is the pressure of the sigma level, and p_t is the constant pressure height of the tropopause set at 100 mb, and π is the terrain pressure defined as

$$\pi \equiv p_s - p_t \tag{2.2}$$

The surface pressure, p_s, was set at 1013 mb initially. The vertical boundary conditions are $\frac{d\sigma}{dt} = 0$ at $\sigma = 0$, ($p = p_t$) and $\sigma = 1$, ($p = p_s$).

C. SPECIFICATIONS OF HEATING AND DAMPING

To evaluate the effect of fluctuating heating as suggested by Holton and Colton (1972), two controlled experiments are carried out. In both experiments the heating function, H, contains two components:

$$H = H_s + H_{AS} \tag{2.3}$$

where H_s, the zonally symmetric heating, is given by a continuous adjustment to a specified equilibrium temperature, T^*, using the following formula,

$$H_s = -\left[\frac{T - T^*(y,\sigma)}{\tau}\right] \tag{2.4}$$

Here T is the temperature and τ is a specified adjustment time set to two days in this study. The equilibirum temperature, T^*, is prescribed to maintain the zonal mean north-south temperature gradient.

The horizontal distribution of heating is derived from the 200 mb time-mean divergence field observed by Krishnamurti (1970) as follows:

$$Q(°K\ day^{-1}) = \text{Divergence}\ (sec^{-1}) \times 10^6 \tag{2.5}$$

The field is smoothed on the boundaries by reducing the strength of the heating by 50% at the points just inside

the boundaries and 80% at the boundary. The entire field was smoothed by a five point space smoother in order to remove small scale features. In the vertical, the full value of heating derived by (2.5) is specified at level 2 and a vertical distribution is assumed such that the heating at level 1 and 3 are 50% and 25%, respectively, of the value at level 2.

The zonally asymmetric component, H_{AS}. takes the following form,

$$H_{AS} = Q \times (1.0 + A(\text{SIN } \frac{2\pi}{T} t)) \qquad (2.6)$$

where A is the amplitude of the heating fluctuation whose period is T. In the first of the two experiments A = 0; in the second, A = 0.5. A 10 to 15 day period was observed by Murakami (1974) and Krishnamurti and Bhlame (1976) in the northern summer monsoon. Here ten days is chosen for the periodicity T for the sake of computation economy.

Linear damping terms are included in the momentum equations to represent the effect of scale-independent friction. Horizontal diffusion is also introduced to include the effect of scale-dependent friction for it damps the small scale fields, which are generated by the finite difference scheme in the model.

D. INTEGRATION SCHEME AND INITIAL CONDITIONS

The time integration is comprised of continuous sections of one Matsuno step and four leapfrog steps, with a time increment of six minutes.

At the onset the pressure levels were initialized at standard heights and temperatures were also specified by the zonally averaged climatology. The model was started without the diabatic forcing function until a quasi-steady circulation was established. At this point the diabatic heating was introduced. For both experiments the model runs for 25 more days from the quasi-steady state with the data of the last 10 days used for computing the time-mean fields. All data presented is interpolated to constant pressure surfaces of 250 mb, 500 mb, and 850 mb.

III. RESULTS

The principal circulation features of the northern summer monsoon are the Tibetan high, the Pacific tropical upper tropospheric trough (TUTT), the tropical easterly jet, the Mexican high and the Atlantic TUTT. The simulation of these features by the model are compared with observations, mainly those by Krishnamurti and Rodgers (1970).

A. TIME MEAN FIELD

1. Steady Heating

The 10 day time-mean fields of wind, geopotential height, temperature and vertical velocity are shown in Figures 4-7. In Figure 4a the 250 mb wind field shows an anticyclonic wind center near 30°N, 52°E which resembles the observed Tibetan high although the position of the generated feature is shifted 30° to the west. The calculated Pacific TUTT extends from 120°W, 40°N to 180°W, 20°N, approximately the same position as the observed TUTT. The TUTT has a northeast-southwest tilt and the amplitude is slightly greater than that observed. The strongest easterly jet is developed by the model in the southern periphery of the Tibetan anticyclone. The jet maximum is located at approximately 60°-90°E, 10°N, with a speed of 22 ms^{-1} which is an underestimate of the observed maximum speed of ~30 ms^{-1}.

The Mexican anticyclone is centered near 130°W, 25°N. This feature is again shifted to the west of the observed

position by 25°. The amplitude of the disturbance compares well with the observed.

The Atlantic TUTT, situated in the mid-Atlantic in the area of 15°N-40°N, 20°-60°W is well developed but again the amplitude is slightly larger than that observed. As for the Pacific TUTT, there is no apparent phase shift problem when compared to observations.

There are no good observational data with which to compare the 500 mb flow shown in Figure 4b. The 850 mb flow (Figure 4c) clearly shows the low-level cyclonic flow below the upper-level Tibetan and Mexican anticyclones. Westward phase shifts of circulation centers also occur at low level and is consistent with the upper level flow.

In Figure 5a, the 250 mb geopotential, the Tibetan and Mexican highs are the main features. The Pacific and Atlantic TUTTs are weak in comparison to observations but well defined.

Figure 6a, the 250 mb temperature field, shows that the Tibetan and Mexican highs are warm core systems. The TUTTs in both the Pacific and Atlantic are clearly indicated by cold regions. These temperature anomalies are present throughout the vertical in both the 500 mb field (Figure 6b) and the 850 mb field (Figure 6c).

As expected, Figure 7, which shows the 400 mb vertical velocity closely resembles the horizontal diabatic heating distribution. This is consistent with the warm core energetics of the monsoon in which the long wave kinetic

energy is converted from the available potential energy generated by diabatic heating.

Figures 8 and 9 show the mean divergence and vorticity fields, respectively. The 250 mb divergence (Figure 8a) is a reasonable reproduction of the 200 mb divergence field as observed by Krishnamurti. This indicates that the specified heating function is properly chosen for simulating the forcing. The vorticity fields are representative of the wind fields shown in Figure 4. A negative vorticity belt surrounds the globe from 8°-25°N. The two TUTTs are clearly shown by fingers of positive vorticity extending into the negative vorticity belts.

2. Fluctuating Heating

The 10-day mean fields of the fluctuating heating forcing function are Figures 10-15. Only the 250 mb level of all the fields is shown except in the cases of vertical velocity (Figure 13) and the time-mean wind fields (Figures 10a,b,c). A close comparison of these fields with the time-mean fields for the steady heating case could not reveal any significant differences between the two cases. The phase shifts of the Tibetan and Mexican highs are almost exactly duplicated by the fluctuating heating, resulting in almost identical amplitudes and phases as those for the steady heating.

The above results suggests that the effect of fluctuating divergence forcing in the summer monsoon suggested by Holton and Colton is not prominent enough to explain the phase problem in the diagnostic simulation of the time-mean

field. This conclusion is true if the amplitude of the fluctuating component in our model is representative of the actual observed amplitude. Since limited observational knowledge (based on Krishnamurti, 1970) does indicate that the actual amplitude of fluctuation may not be much larger than what is specified here, Holton and Colton's hypothesis seems unlikely to be valid.

B. TRANSIENT FIELD

The second purpose of this study is to examine the synoptic-scale transient disturbances associated with the planetary-scale monsoon circulation.

1. Steady Heating

Figure 16 is a time-longitude section for the 12-hour interval 200 mb vorticity field at 12°N from day 15 to day 25. In the western hemisphere from 0°-90°W there is evidence for strong synoptic-scale westward-propagating wave activity. The wavelengths of these disturbances vary from 3500 km at 30°W to 2200 km at 60°W. In some cases the wavelength can be as short as 1000 km at 180°W to 90°E where the disturbances appear to be much more irregular with long wavelengths at the beginning of the time series and sporatic, short wavelengths toward the end.

Upstream from the jet maximum near 50°E the disturbance activity is very minimal with small amplitude. The waves begin to grow in the area of the easterly jet maximum and continue to grow as they propagate westward. Downstream of

the easterly jet maximum the synoptic waves appear to be much more organized comparing to upstream of the jet.

Krishnamurti (1971) and Colton (1972) have found that the upper-level synoptic waves are largely due to the barotropic instability associated with the easterly jet. To examine this possibility as the generation mechanism of the waves observed in this model, we plot the meridional gradient of the basic absolute vorticity

$$\beta - \frac{\partial^2 \bar{u}}{\partial y^2} ,$$

where β is the gradient of the coriolis parameter and $\bar{u}$ is the time-mean zonal wind component, as a function of x and y in Figure 17. It is obvious that the sign of this quantity changes within the north-south channel throughout the domain. Thus it is quite probable that the barotropic instability exists everywhere at the 250-mb level. The important role played by the easterly jet in this regard is reflected by the fact that the entire latitude band of 12°N has negative values for this quantity.

The result that the wave amplitude is minimum upstream of the easterly jet and increases to a maximum downstream further suggests that the mean kinetic energy is converted into eddy kinetic energy in the vicinity of the easterly jet maximum. There should be a stable area upstream of the easterly jet maximum where the amplitude of the disturbances is small. The amplitude near the jet maximum may be small but the change in amplitude is large as the wave

propagates past the jet indicating that the jet maximum is the most unstable region. This result indicates that the most active area for synoptic-scale wave disturbances is in the Atlantic, Caribbean and Central America, not in the Pacific and Indian Ocean areas. There are two possible factors in the model that influence this: (1) The model position of the Tibetan high is shifted by 30° to the west from the observed position, and there is a corresponding shift in the jet maximum from the Indian to the Arabian Sea. The most active wave region should be downstream from the jet maximum so this region is shifted from the Arabian Sea and Africa to the Atlantic area. Also the Atlantic TUTT has been known to be an active area for upper-level cold core lows to develop. It is possible that the synoptic waves observed here are also a reflection of the cold core lows. On the other hand, the absence of strong disturbance activity in the Pacific TUTT region, in contrast to the finding by Colton (1972), may also be explained by the westward phase of the easterly jet maximum. (2) This model contains a horizontal diffusion which tends to reduce the zonal wind shear and in so doing the barotropic instability. This diffusion was not used by Colton (1972). It is noteworthy, however, that even in this model the barotropic instability mechanism is still found to be prominent downstream from the jet maximum. An optimum use of the diffusion, to alleviate the problem associated with the finite differencing and at the same time avoid strong artificial smoothing of the basic

wind shear, should give us a better simulation of this mechanism.

As an example for the barotropically unstable wave, a sequence of 12-hour interval 250 mb wind analysis is shown in Figures 18 a-d, from 0000 GMT, day 22 to 1200 GMT day 23. Here we shall follow the development of three waves in time. Their positions at 80°W, 4°-16°N; 60°W, 4°-16°N and 30°W, 4°-16°N on 0000 GMT day 22 are indicated by dashed lines. As time progresses each wave propagates to the west with a wavelength of ~3500-4000 km. The meridional tilt of the depicted waves is approximately northwest-southeast. From Figure 4a, the maximum time-mean easterly zonal wind is near 12°N in the vicinity of the waves in question. Thus in the 12°-16°N band the time-mean zonal wind has a northeast-southwest shear which opposes the wave tilt. This is clearly another indication that the waves are barotropically unstable.

2. Fluctuating Heating

Figure 20 shows the time-mean meridional gradient of the absolute vorticity for the fluctuating heating case and, as expected, strongly resembles Figure 17 for the steady heating case. There is no question on the plausibility for barotropic instability to exist.

The time-section of the mean vorticity, Figure 19, also points out that the greatest wave activity is downwind of the maximum jet. The amplitude of the waves, however, appears to be greater in this fluctuating heating case, though

the range of wavelengths remains the same as the steady heating case. There is also no noticeable change in phase speed of ~7.6° day^{-1}. This increase in amplitude is readily apparent in the waves generated in the Atlantic area of 20°-90°W, 8°-16°N. This result indicates that the fluctuation of the total forcing field may actually enhance the barotropic energy conversion. In Figure 21, by following the waves initially located at 85°W, 8°-16°N; 55°W, 10°-16°N and 30°W, 8°-16°N; it is found that the tilt of the waves, northwest-southeast, again opposes the horizontal shear of the basic wind.

IV. CONCLUSIONS

One major conclusion of this study is that the westward phase shift problem of the simulated Tibetan and Mexican highs in the absence of very strong damping is not likely to be explainable by the influence of the fluctuating heating. On the other hand, the tropical upper tropospheric troughs do not exhibit this phase problem. This may indicate the importance of damping due to cumulus transport of momentum and vorticity because cumulus convection is predominant below upper level high pressure areas only.

In this model the upper-level barotropic instability seems to be quite important for most of the area, even though the easterly jet was not developed to the fully observed strength, perhaps due to the inclusion of the somewhat strong horizontal diffusion. This instability seems particularly important when time-fluctuations of the planetary-scale is included through the imposed fluctuating heating. Thus the local barotropic instability at upper levels may be more important than that implied by the horizontal shear of the time-mean wind. Further investigations on this mechanism would be desirable to see whether the observed upper level disturbances, such as the cold core lows, are of this nature. Incorporation of cumulus parameterization and topography in the model should further enable us to study the possible implication of this upper level barotropic instability in the vertical development of other tropical disturbances.

In addition to the phase shift problem, Holton and Colton (1972) also found very large amplitudes for long waves in the case of weak damping in their linear model. Our results do not have this amplitude discrepancy. This indicates that the transient waves due to non-linear barotropic energy conversion serves as an energy sink of the planetary-scale flow.

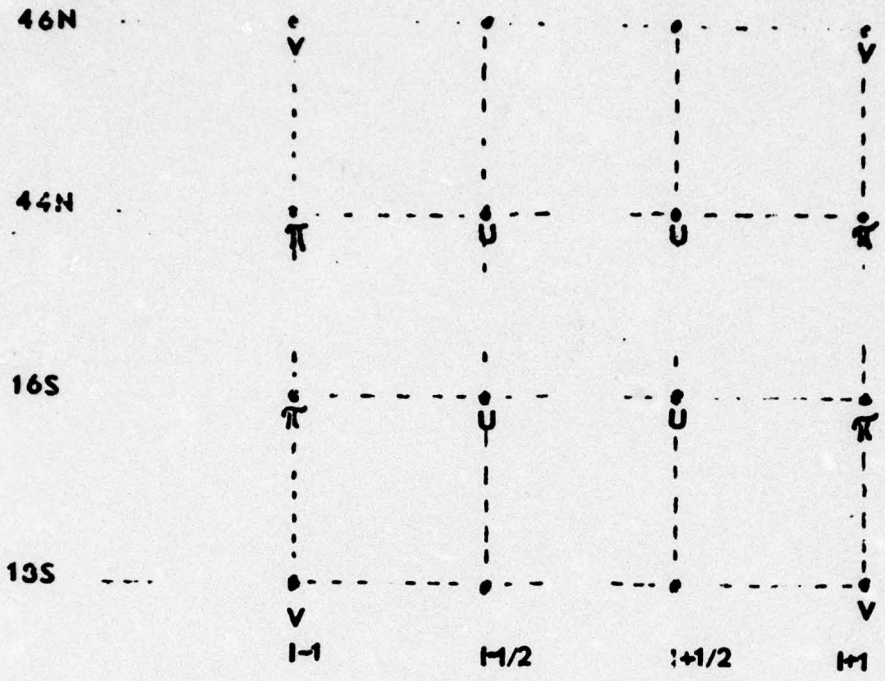

Figure 1. The horizontal distribution of dependent variables. The variables T, Φ, and π are carried at "π-points."

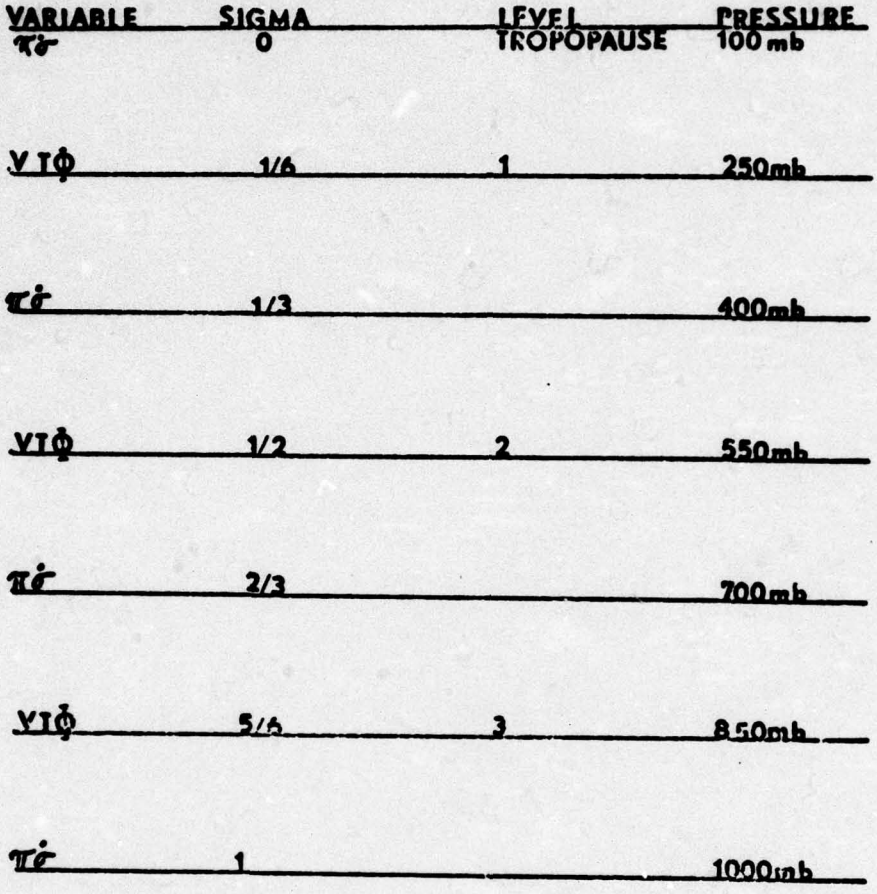

Figure 2. Vertical levels: Sigma is the vertical coordinate. V is the horizontal vector velocity. π is the terrain pressure; T is the temperature and Φ is the geopotential.

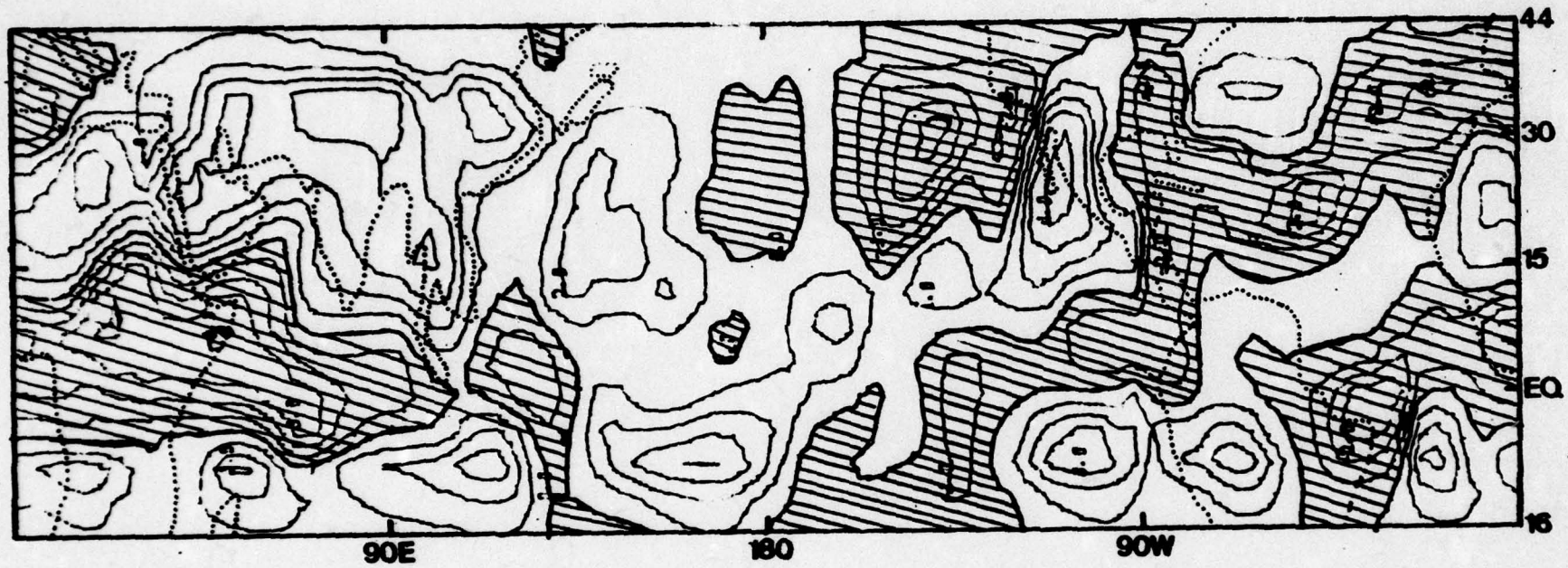

Figure 3. Horizontal distribution of heating. Hatched area indicates negative heating. The interval is 1°K day^{-1}.

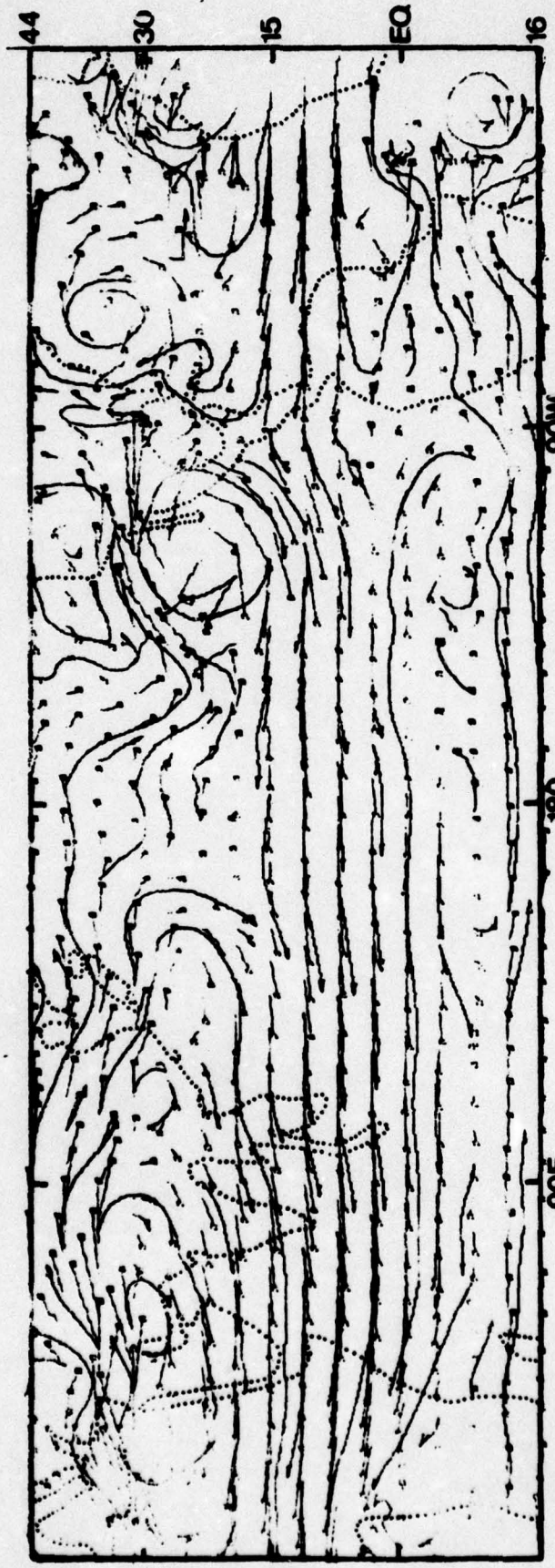

Figure 4a. 250 mb time-mean wind, steady heating.

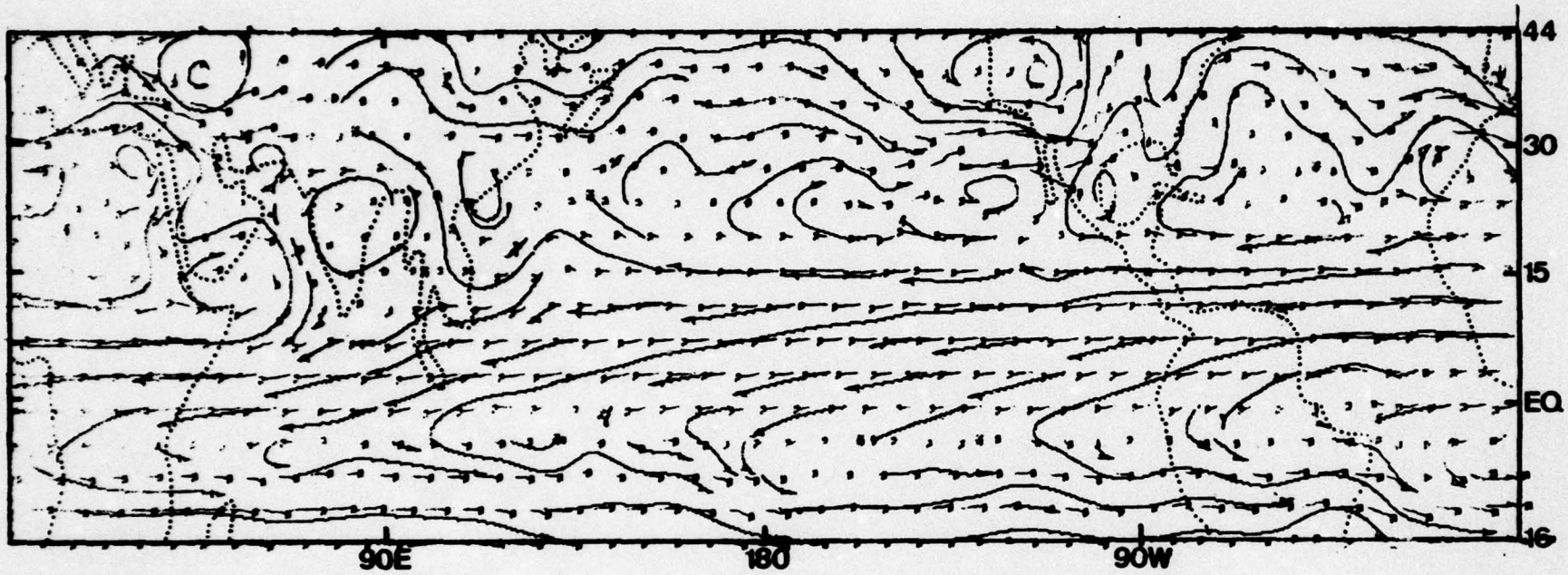

Figure 4b. 500 mb time-mean wind, steady heating.

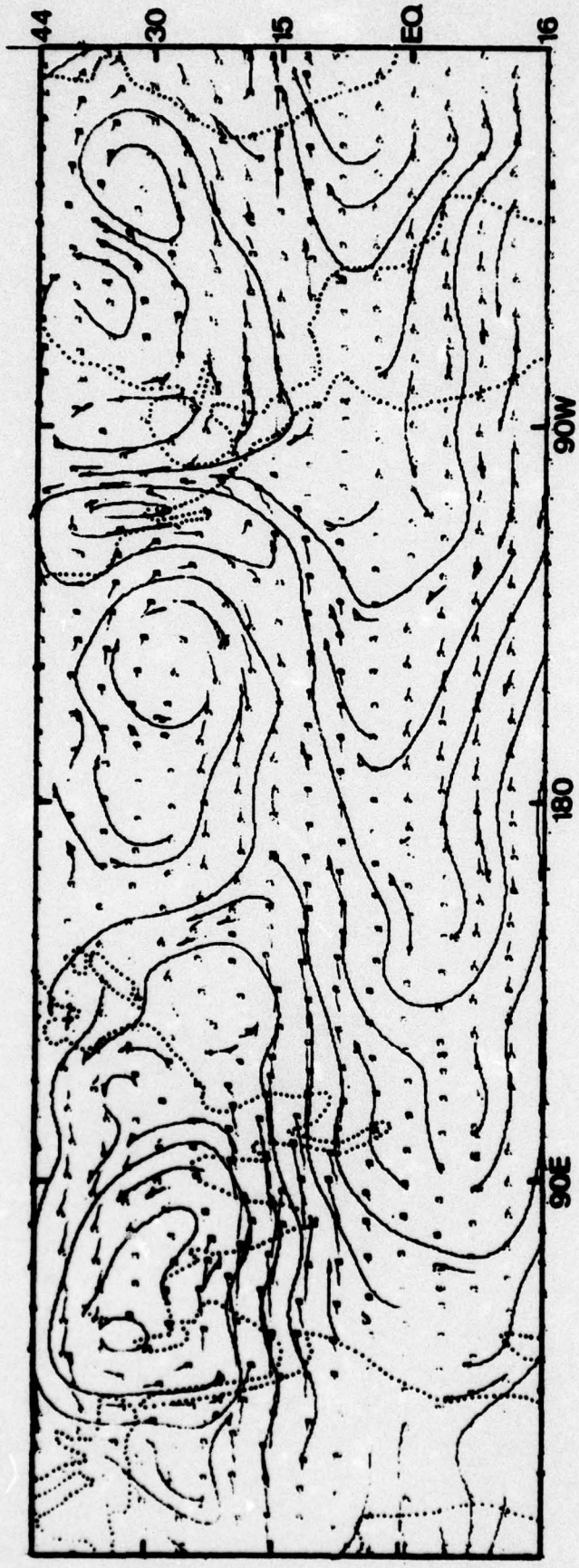

Figure 4c. 850 mb time-mean wind, steady heating.

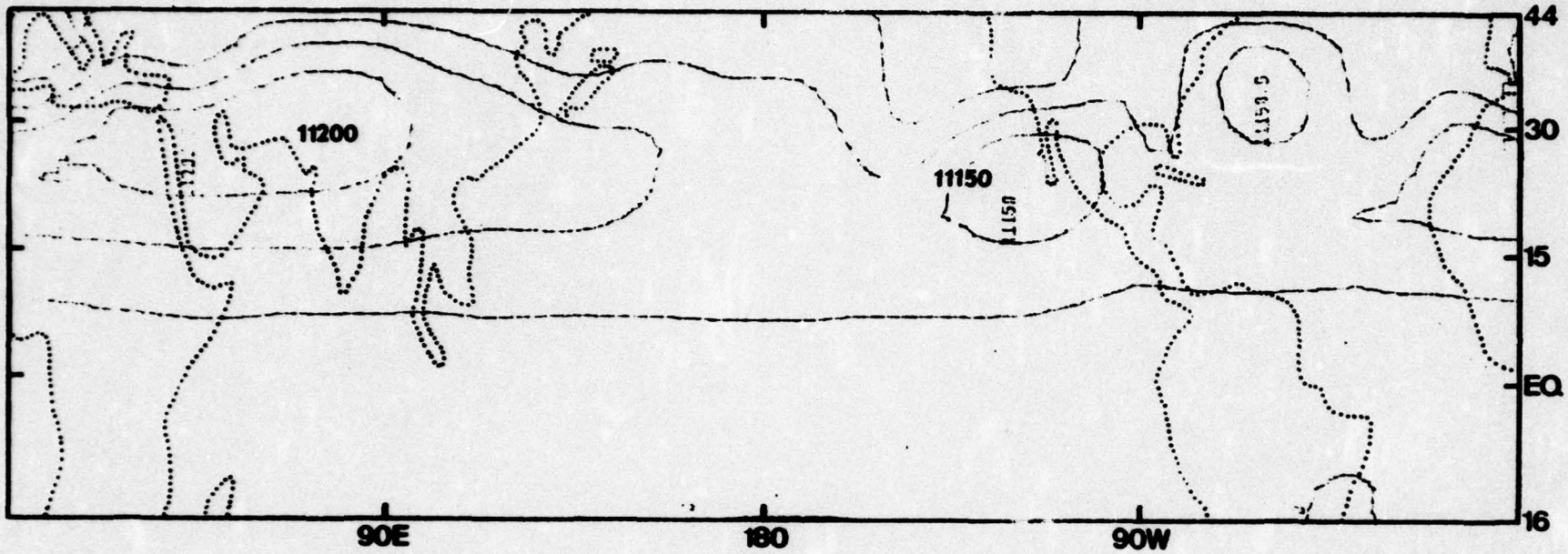

Figure 5a. 250 mb time-mean geopotential field, steady heating. Interval is 50 $m^2 s^{-2}$.

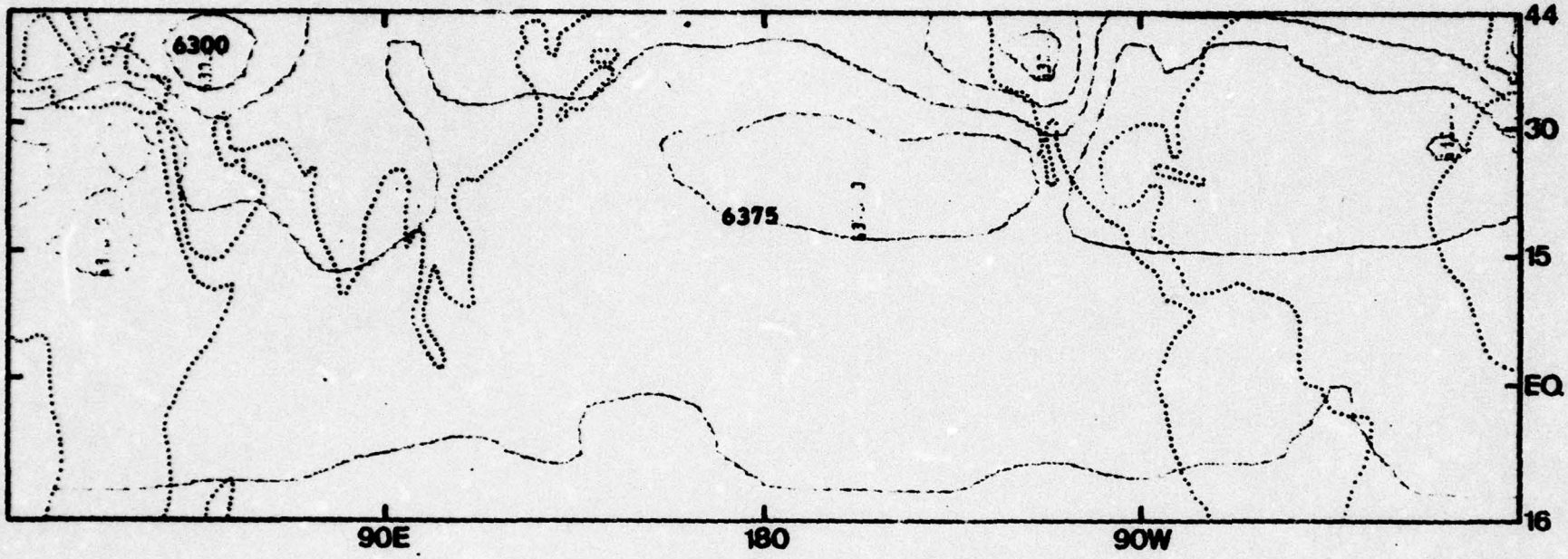

Figure 5b. 500 mb time-mean geopotential field, steady heating. Interval is 25 $m^2 s^{-2}$.

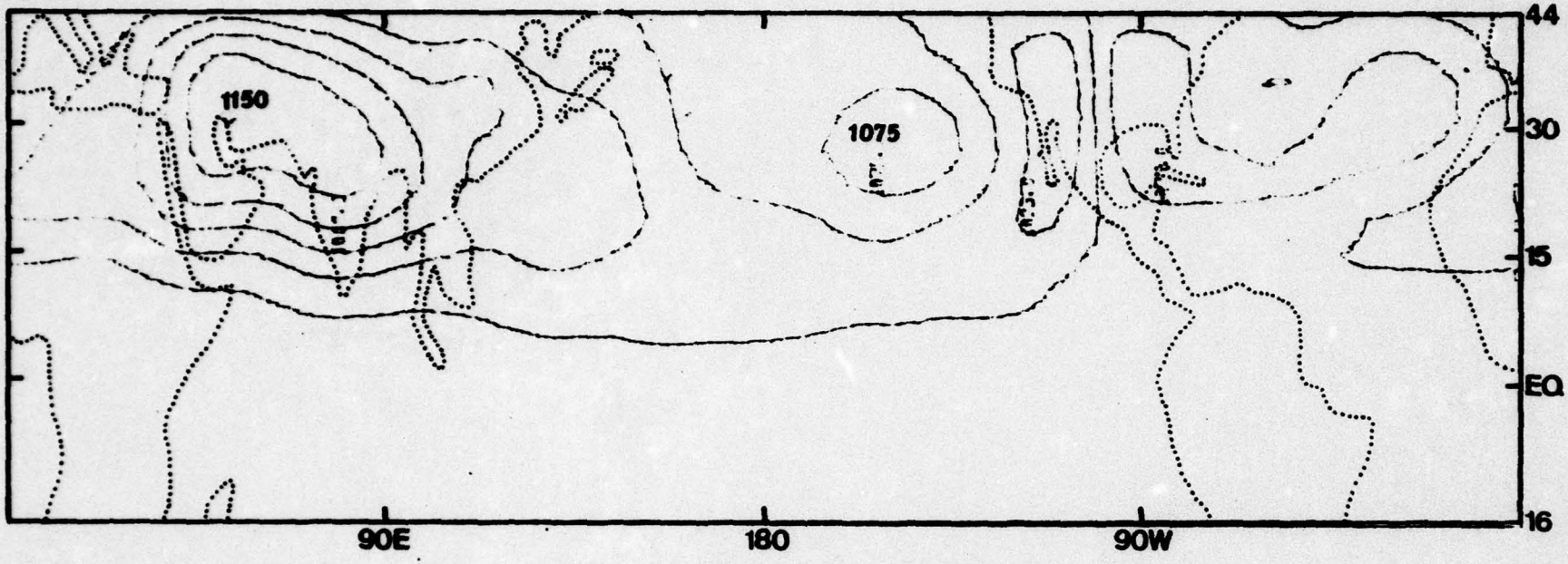

Figure 5c. 850 mb time-mean geopotential field, steady heating. Interval is 25 $m^2 s^{-2}$.

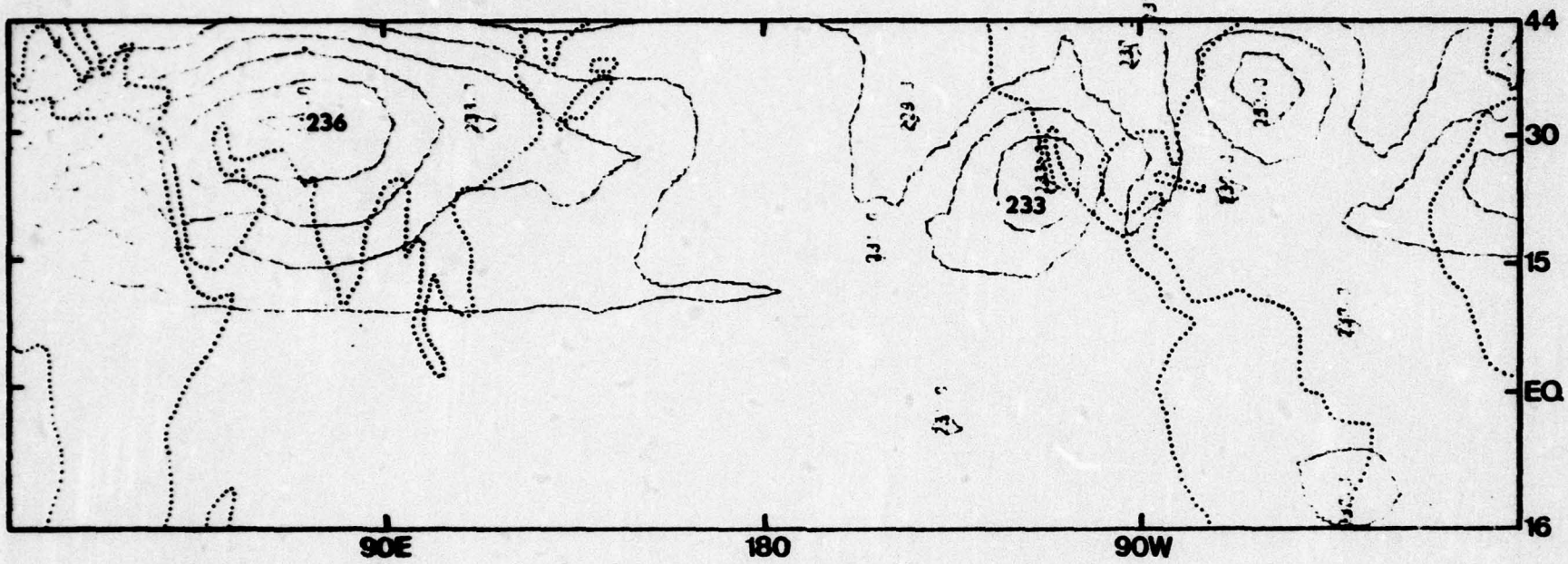

Figure 6a. 250 mb time-mean temperature field, steady heating. Interval is 1°K.

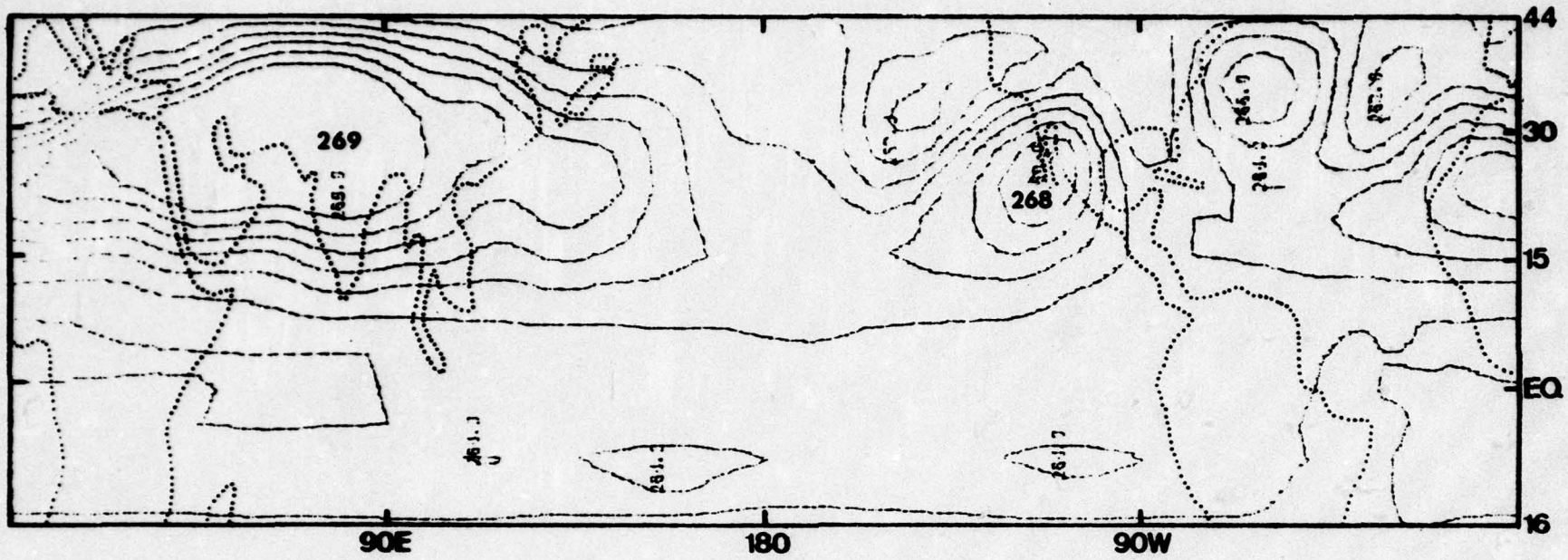

Figure 6b. 500 mb time-mean temperature field, steady heating. Interval is 1°K.

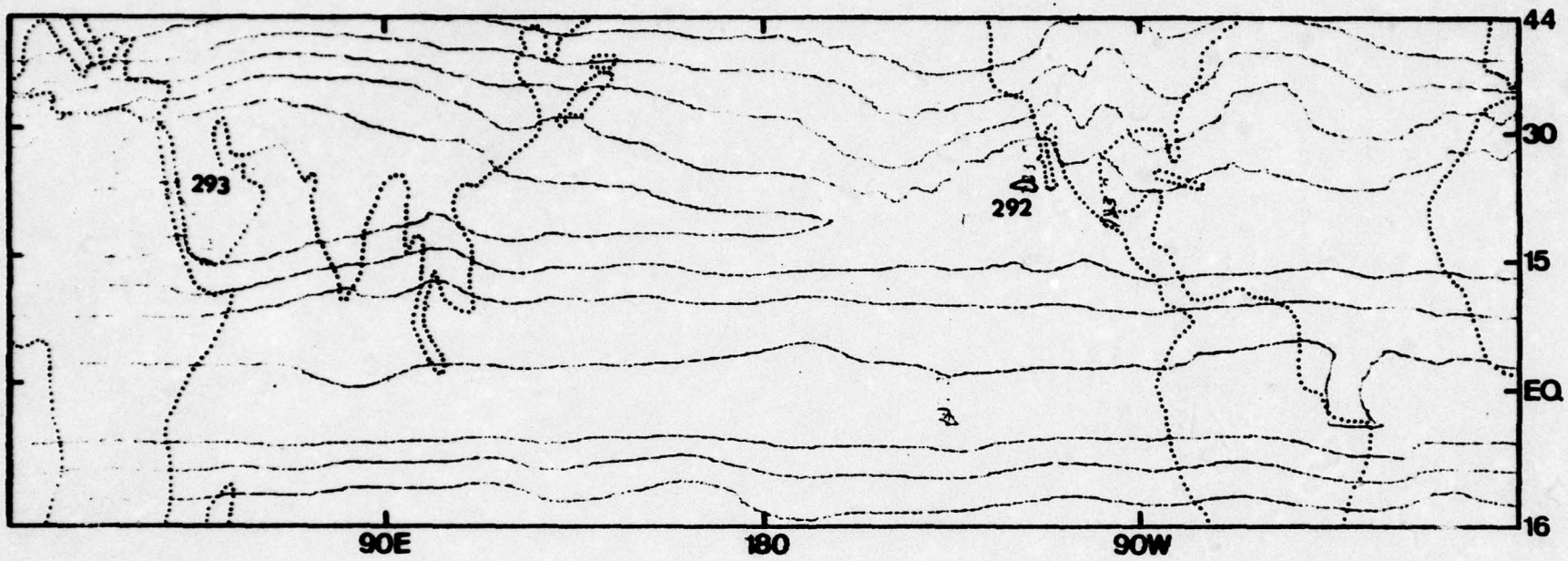

Figure 6c. 850 mb time-mean temperature field, steady heating. Interval is 1°K.

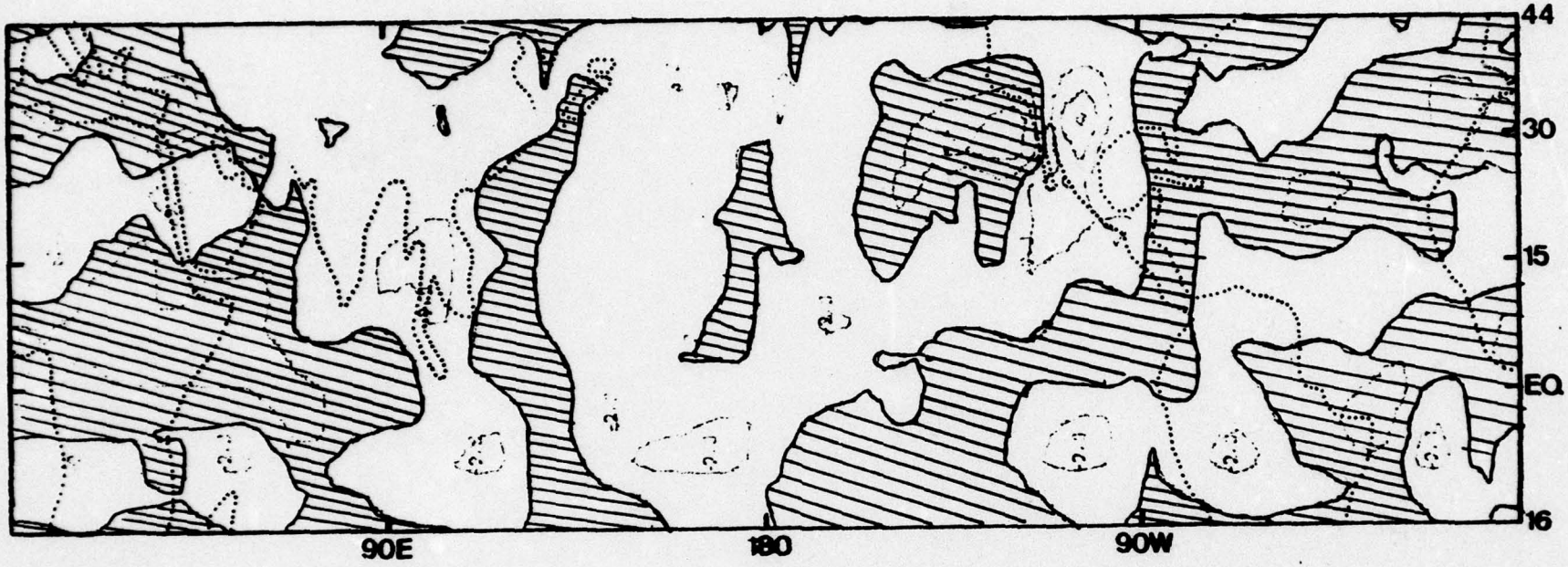

Figure 7. 400 mb time-mean vertical velocity. Hatched area indicates positive value. Interval is 1 mb hr^{-1}.

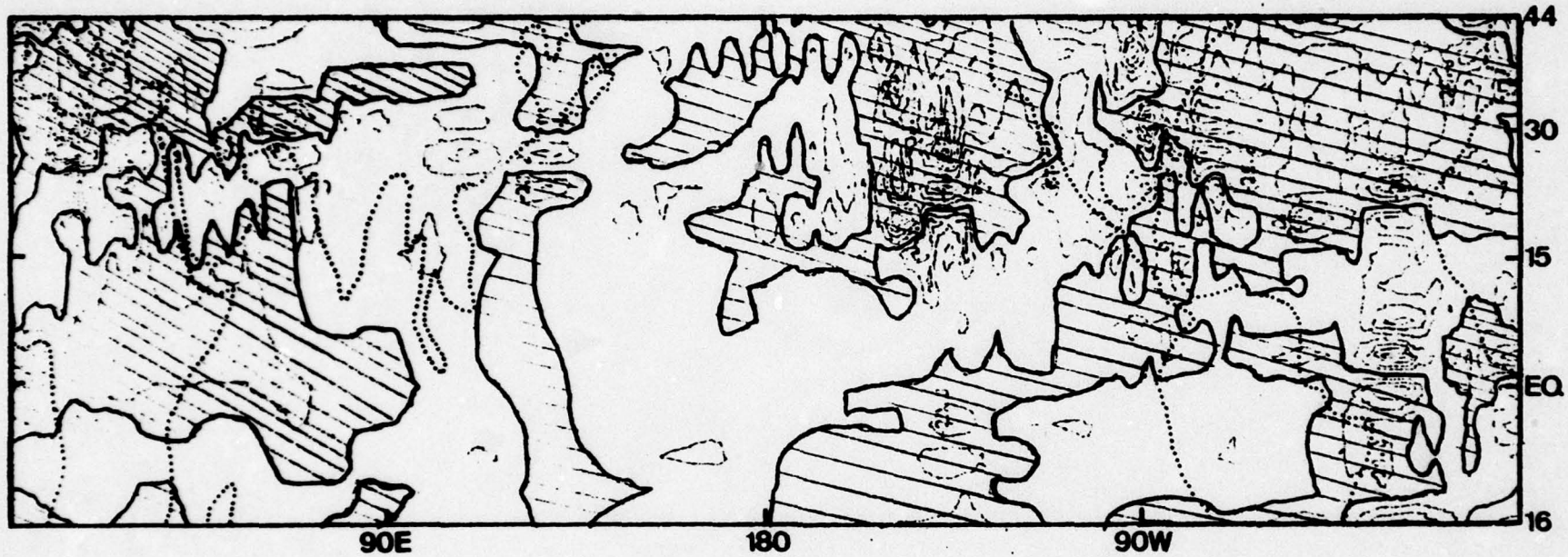

Figure 8a. 250 mb time-mean divergence, steady heating. Hatching indicates negative values. Interval is $10^{-6}s^{-1}$.

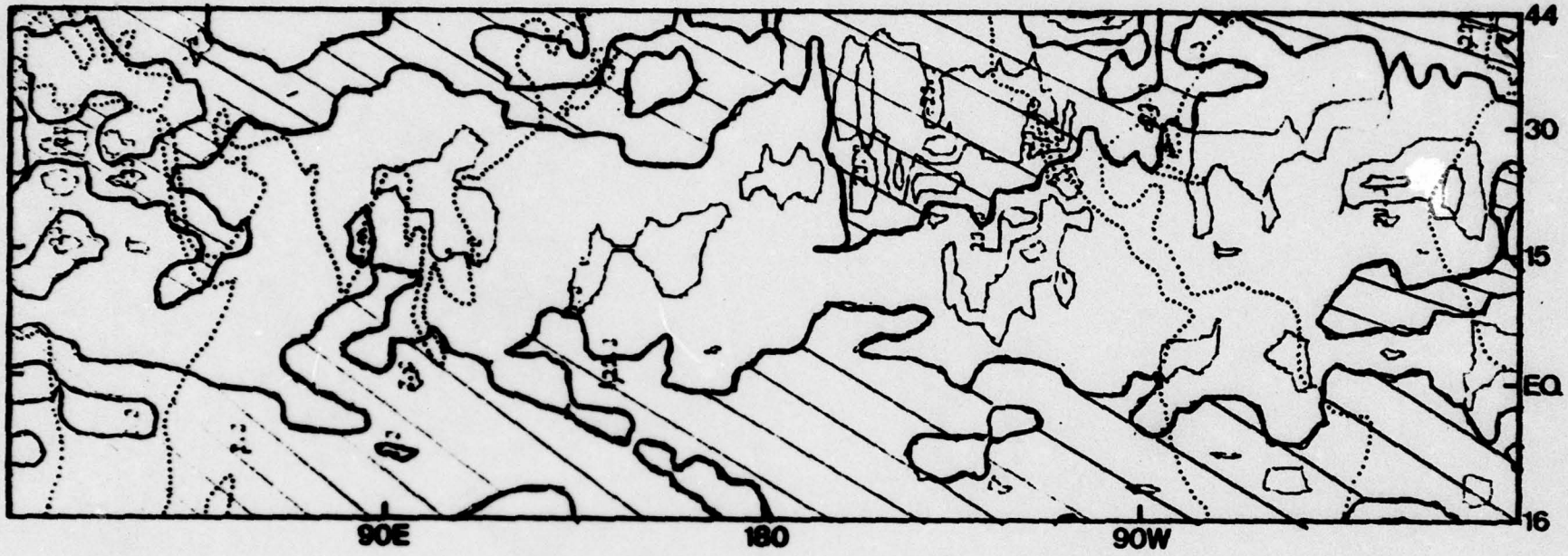

Figure 8b. 500 mb time-mean divergence, steady heating. Hatching indicates negative values. Interval is $10^{-6}s^{-1}$.

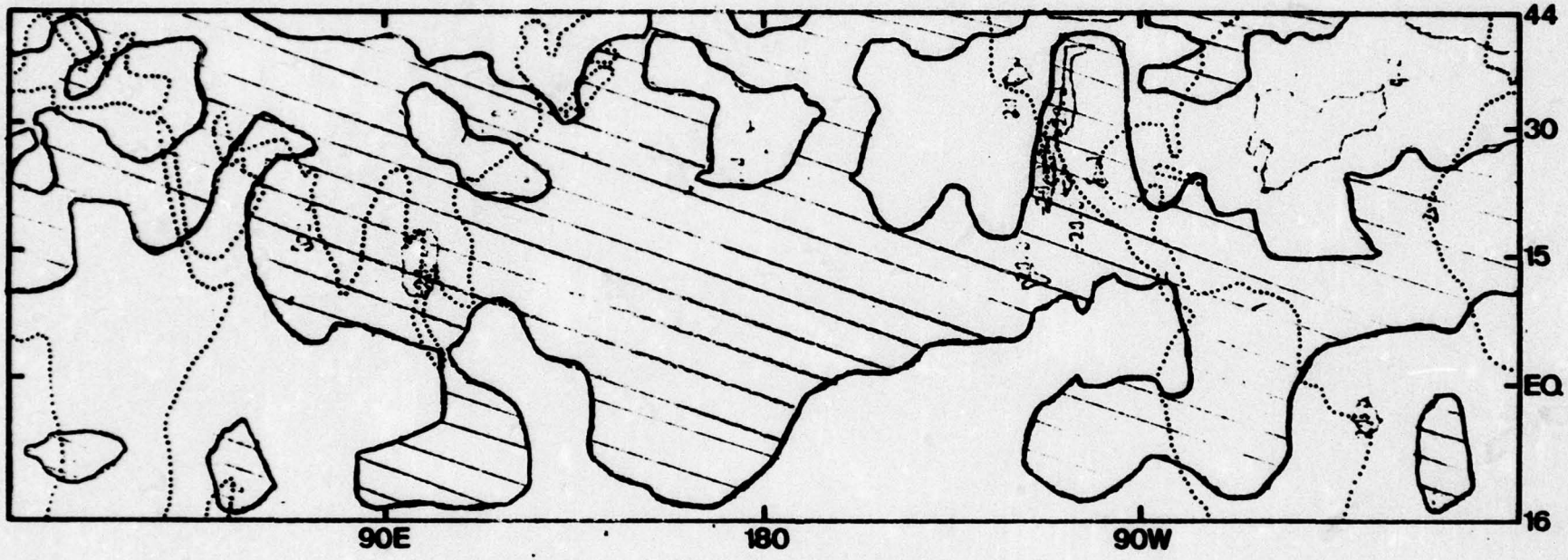

Figure 8c. 850 mb time-mean divergence, steady heating. Hatching indicates negative values. Interval is $10^{-6}s^{-1}$.

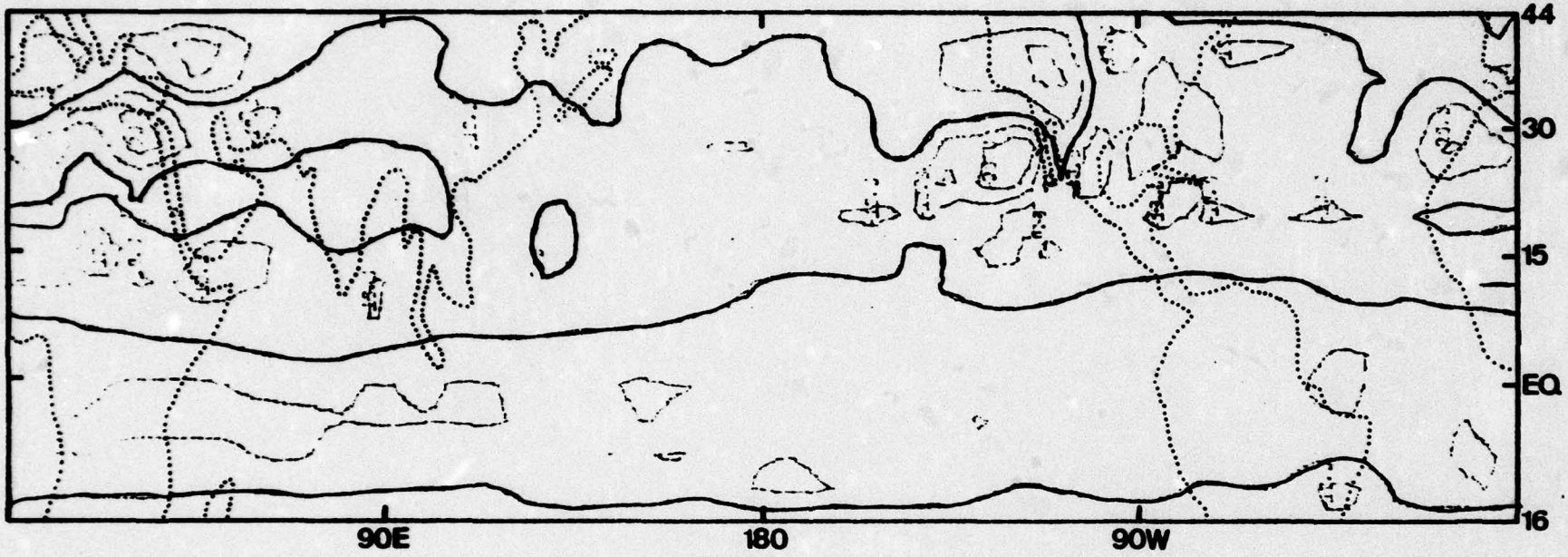

Figure 9a. 250 mb time-mean vorticity, steady heating. Interval is $10^{-5}s^{-1}$.

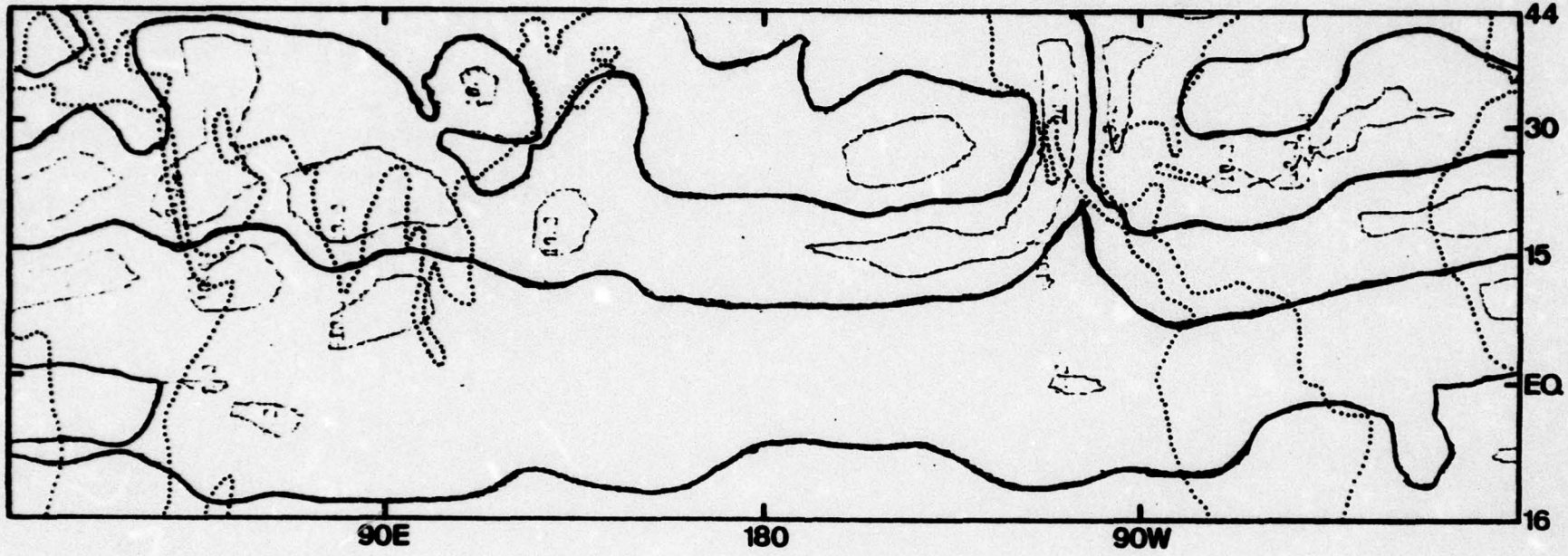

Figure 9b. 500 mb time-mean vorticity, steady heating. Interval is $10^{-5}s^{-1}$.

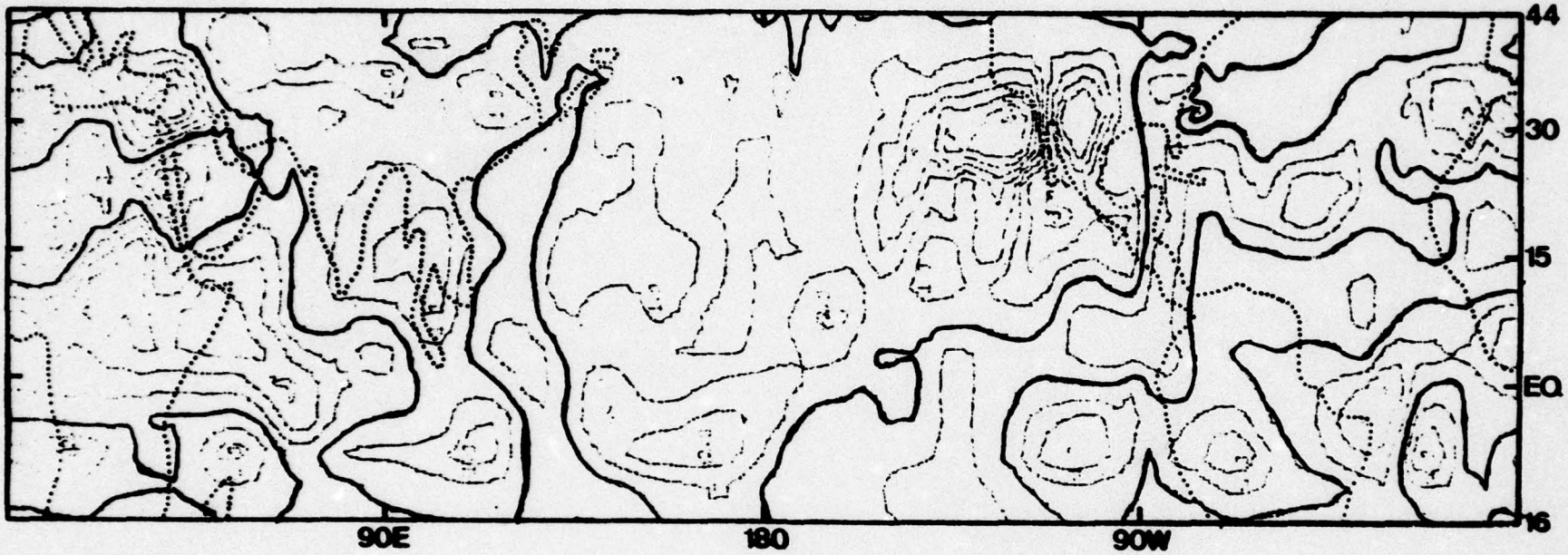

Figure 9c. 850 mb time-mean vorticity, steady heating. Interval is $10^{-5}s^{-1}$.

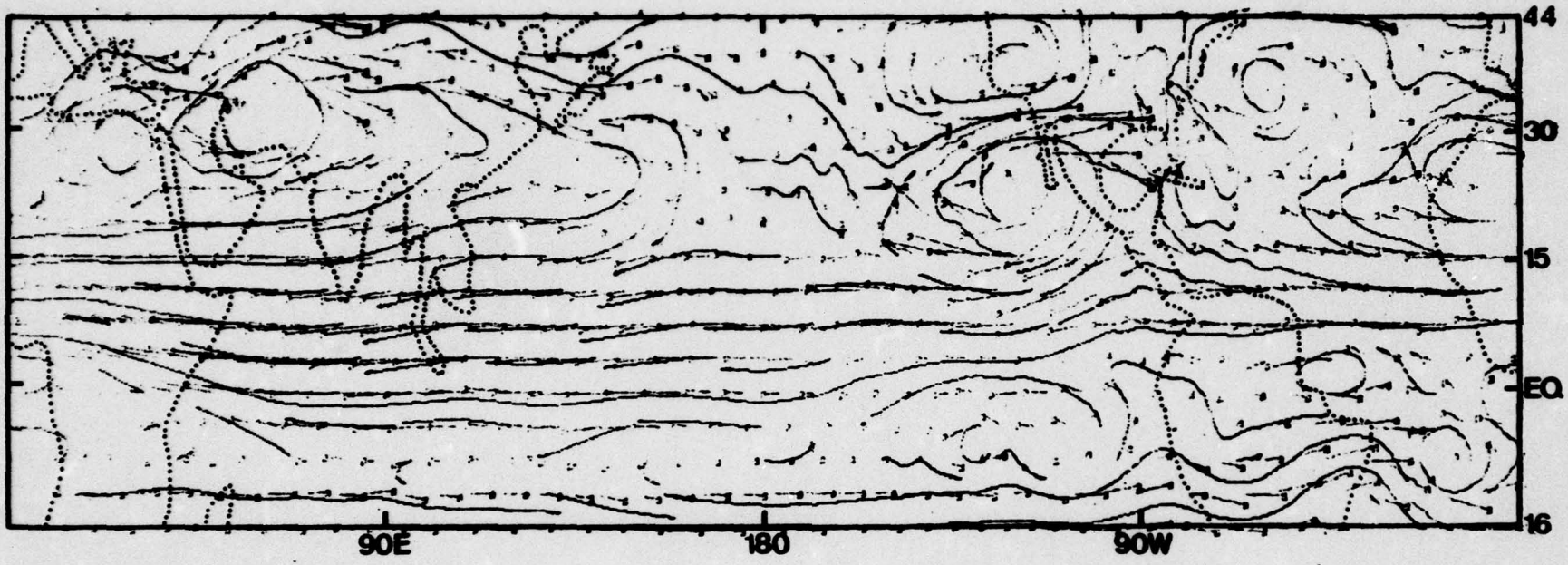

Figure 10a. 250 mb time-mean wind field, fluctuating heating.

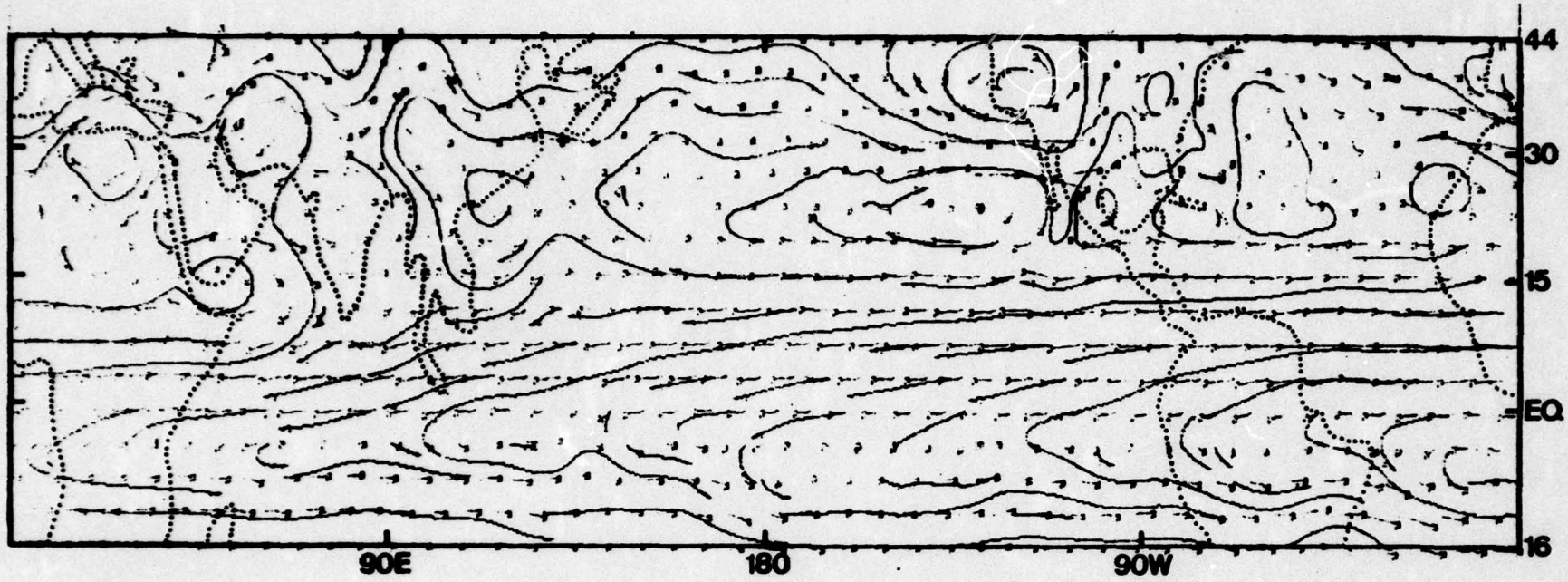

Figure 10b. 500 mb time-mean wind field, fluctuating heating.

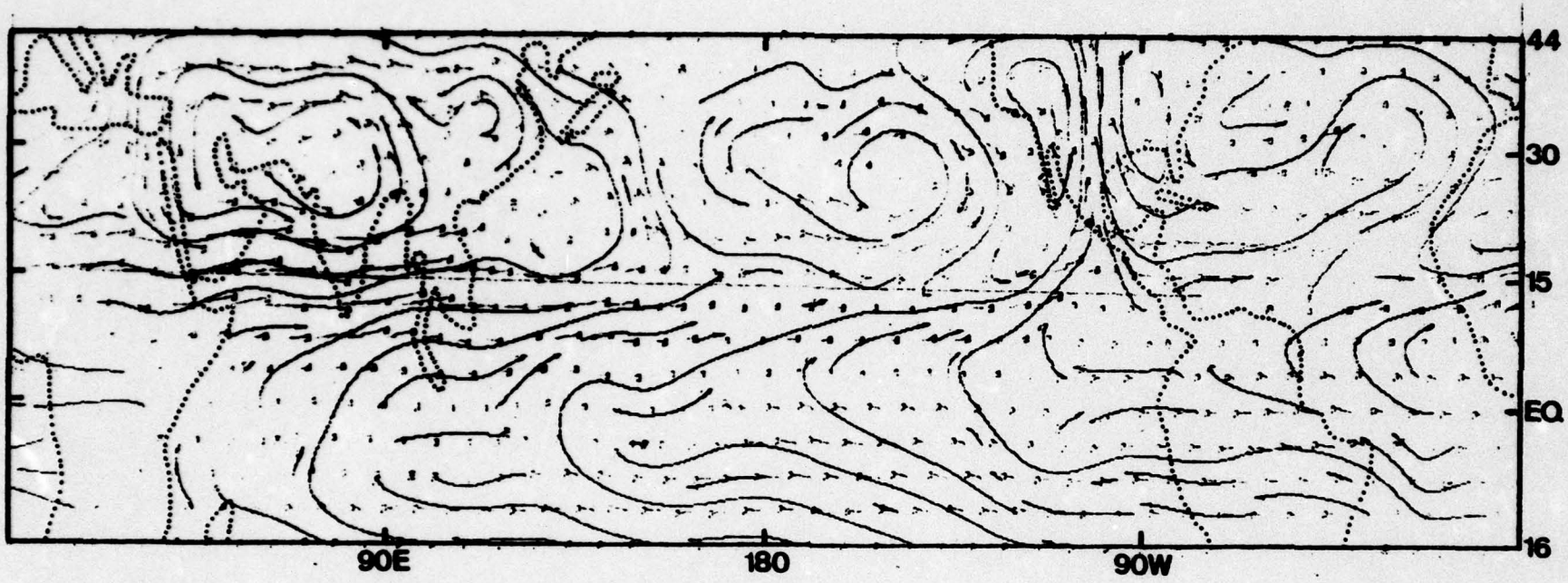

Figure 10c. 850 mb time-mean wind field, fluctuating heating.

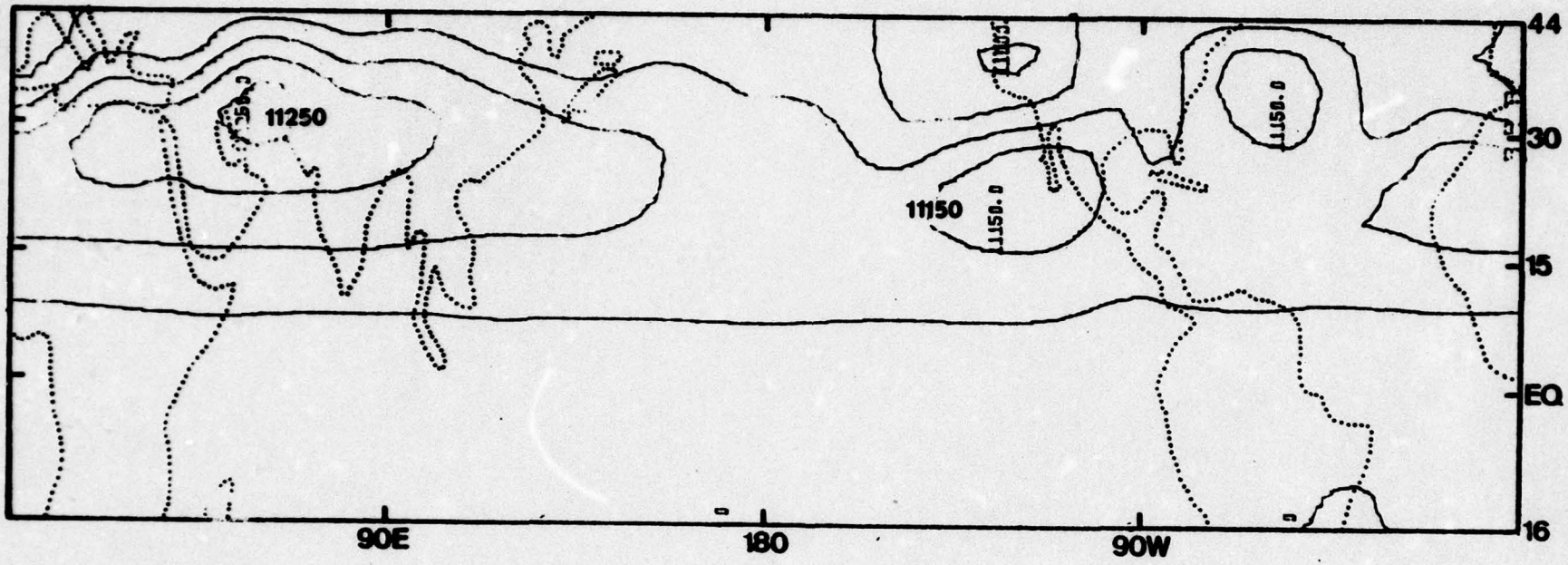

Figure 11. 250 mb time-mean geopotential field fluctuating heating. Interval is 50 $m^2 s^{-2}$.

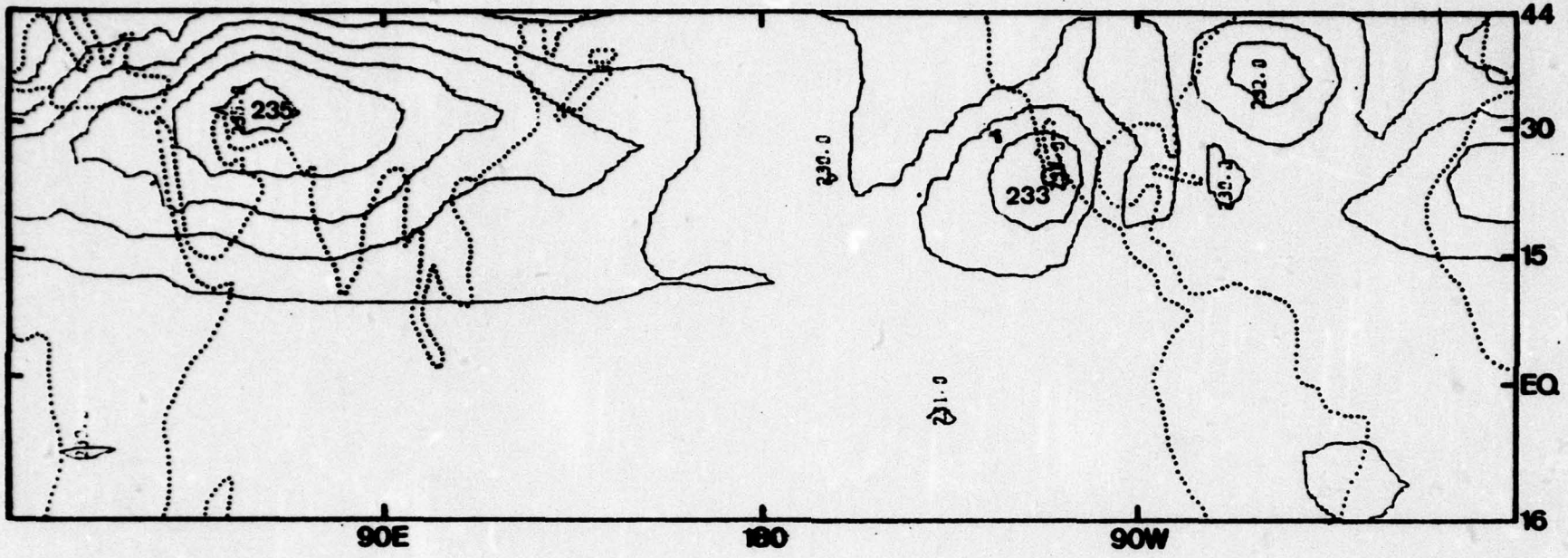

Figure 12. 250 mb time-mean temperature field fluctuating heating. Interval is 1°K.

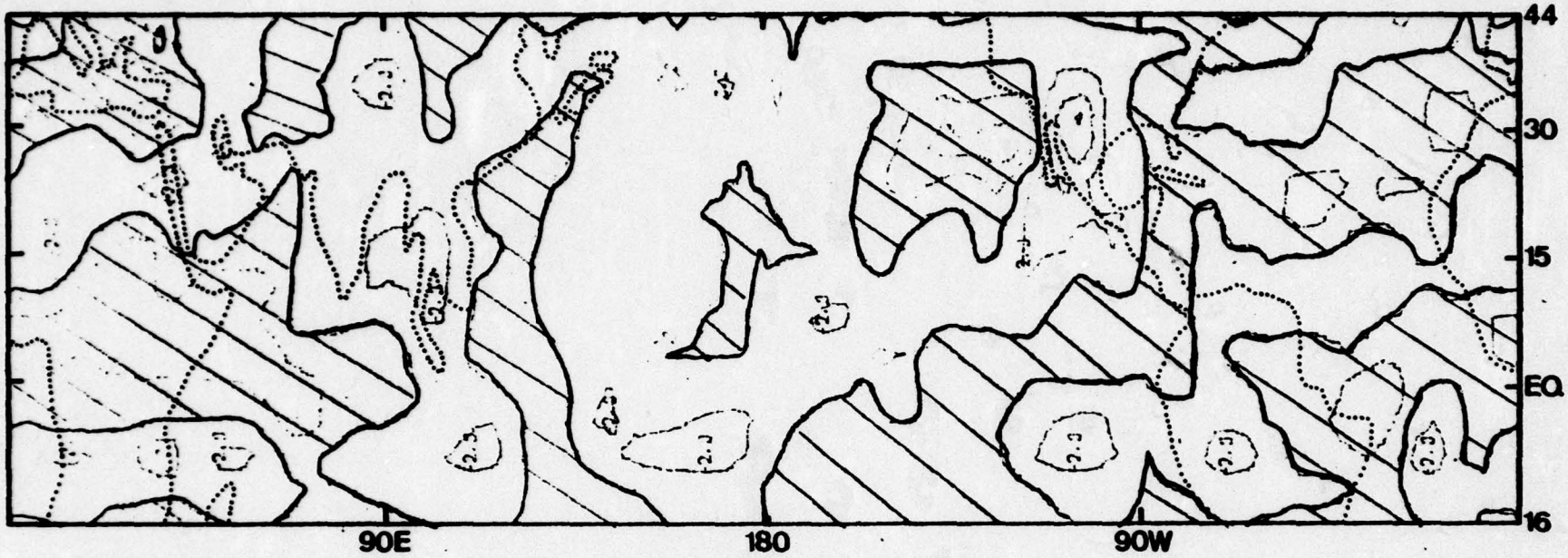

Figure 13. 400 mb time-mean vertical velocity, fluctuating heating. Hatched area indicates positive values. Interval is 1 mb hr^{-1}.

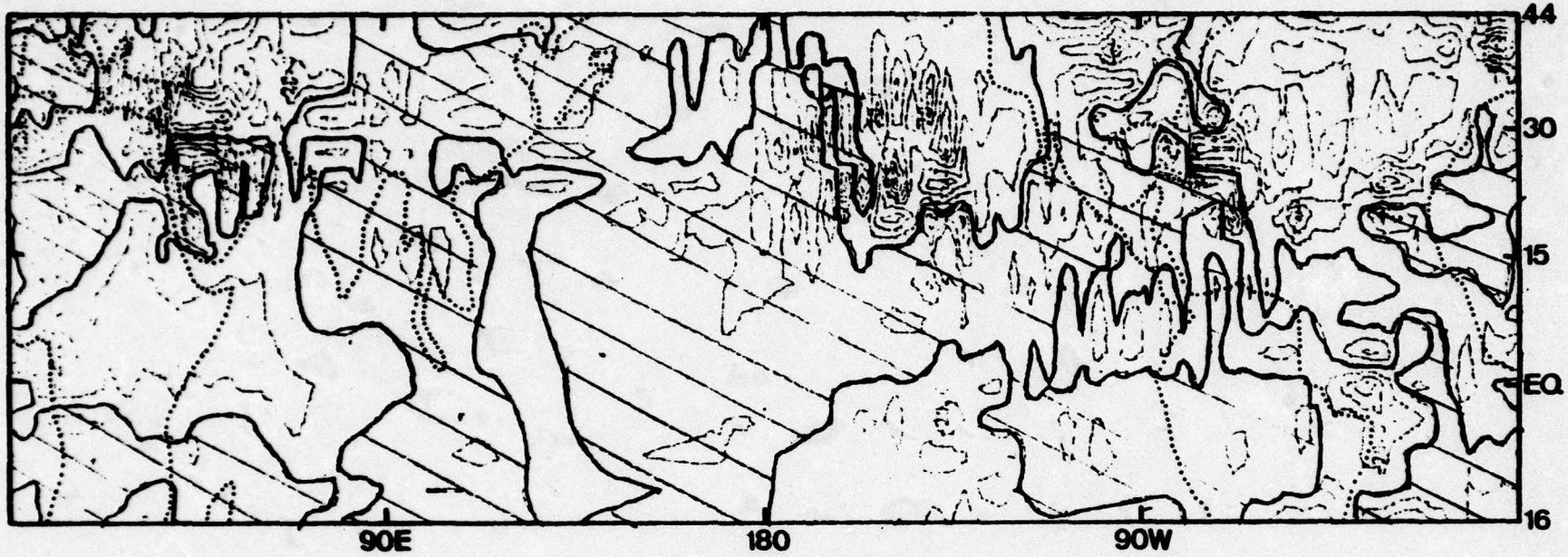

Figure 14. 250 mb time-mean divergence, fluctuating heating. Hatched area indicates positive values. Interval is $10^{-6}s^{-1}$.

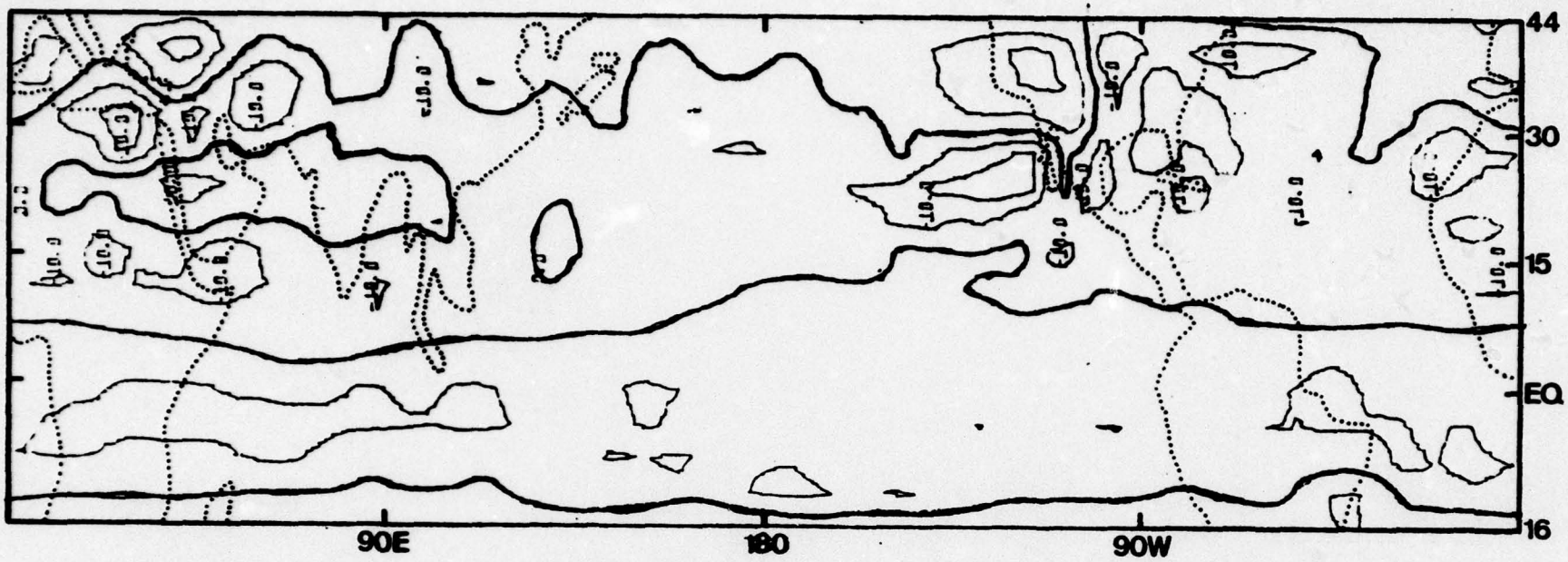

Figure 15. 250 mb time-mean vorticity, fluctuating heating. Interval is $10^{-5}s^{-1}$.

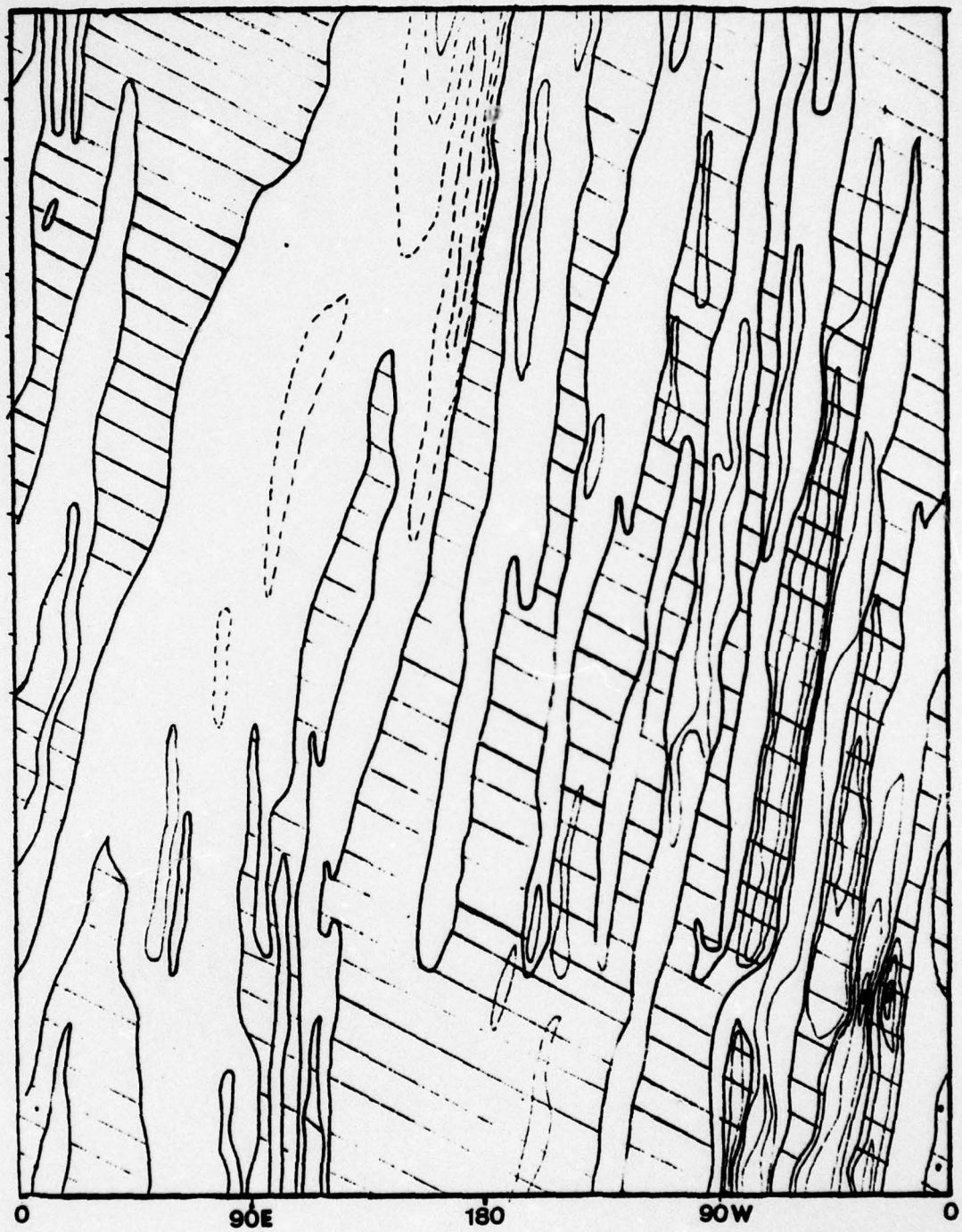

Figure 16. 250 mb vorticity time-longitude section at 12°N, steady heating. Hatched area indicates positive values.

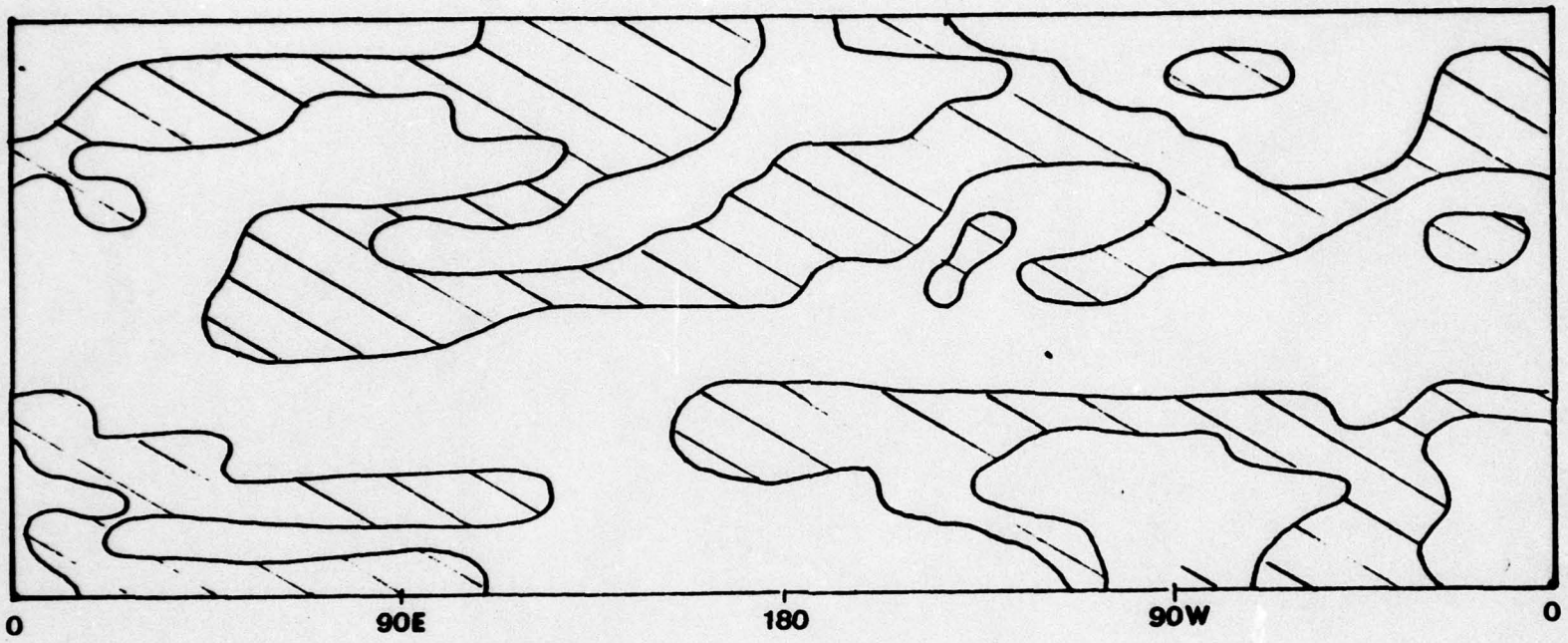

Figure 17. Meridional gradient of basic absolute vorticity, steady heating. Hatched area indicates positive values.

Figure 18a. 250 mb wind, steady heating, Day 22.

Figure 18b. 250 mb wind, steady heating, Day 22.5.

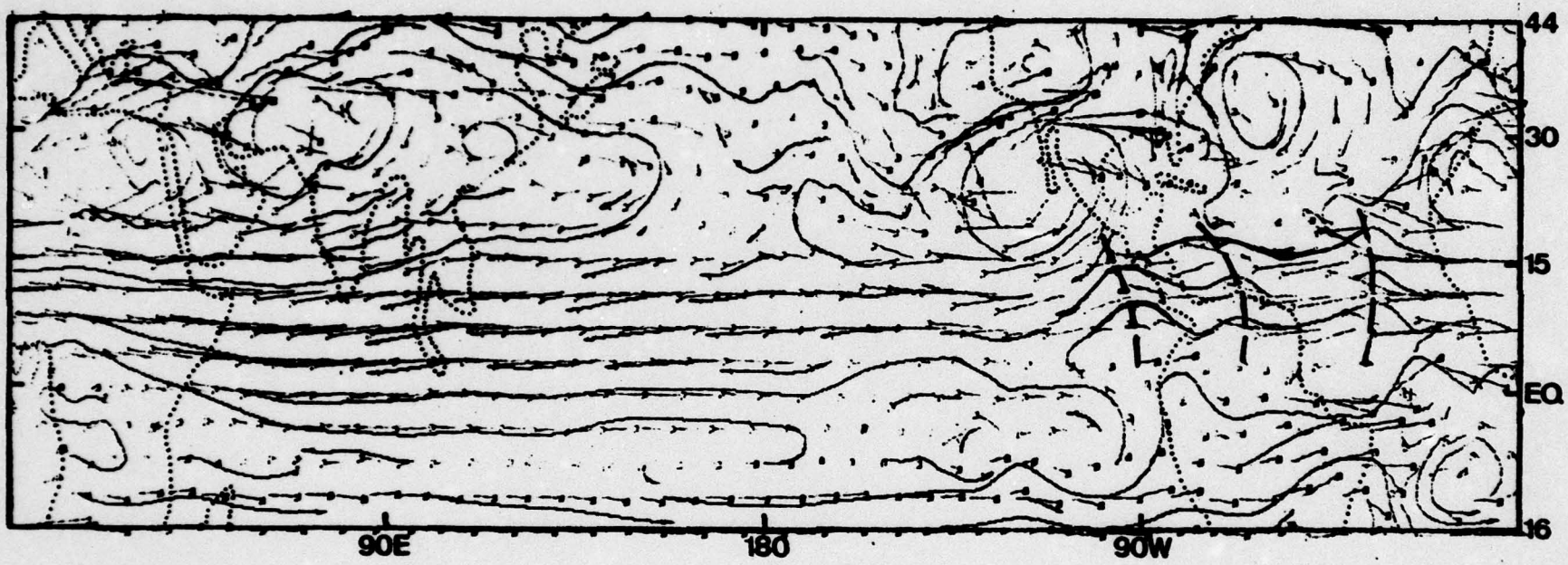

Figure 18c. 250 mb wind, steady heating, Day 23.

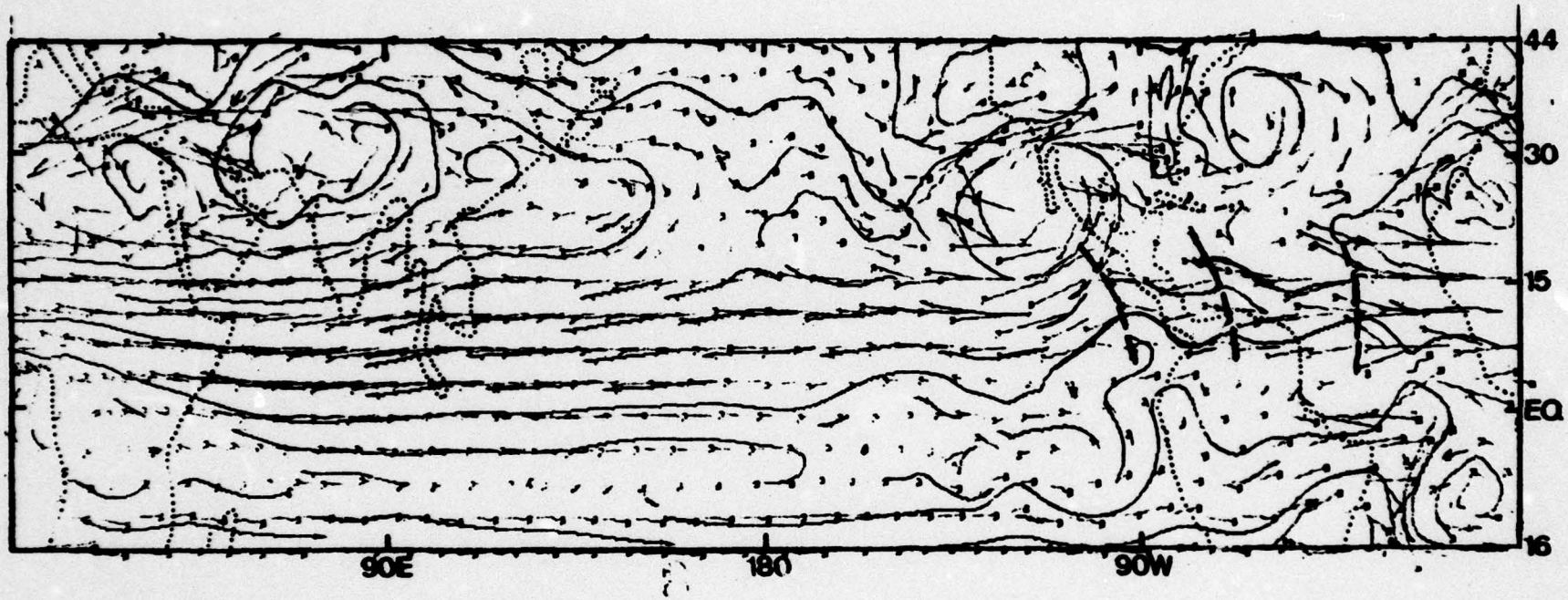

Figure 18d. 250 mb wind, steady heating, Day 23.5.

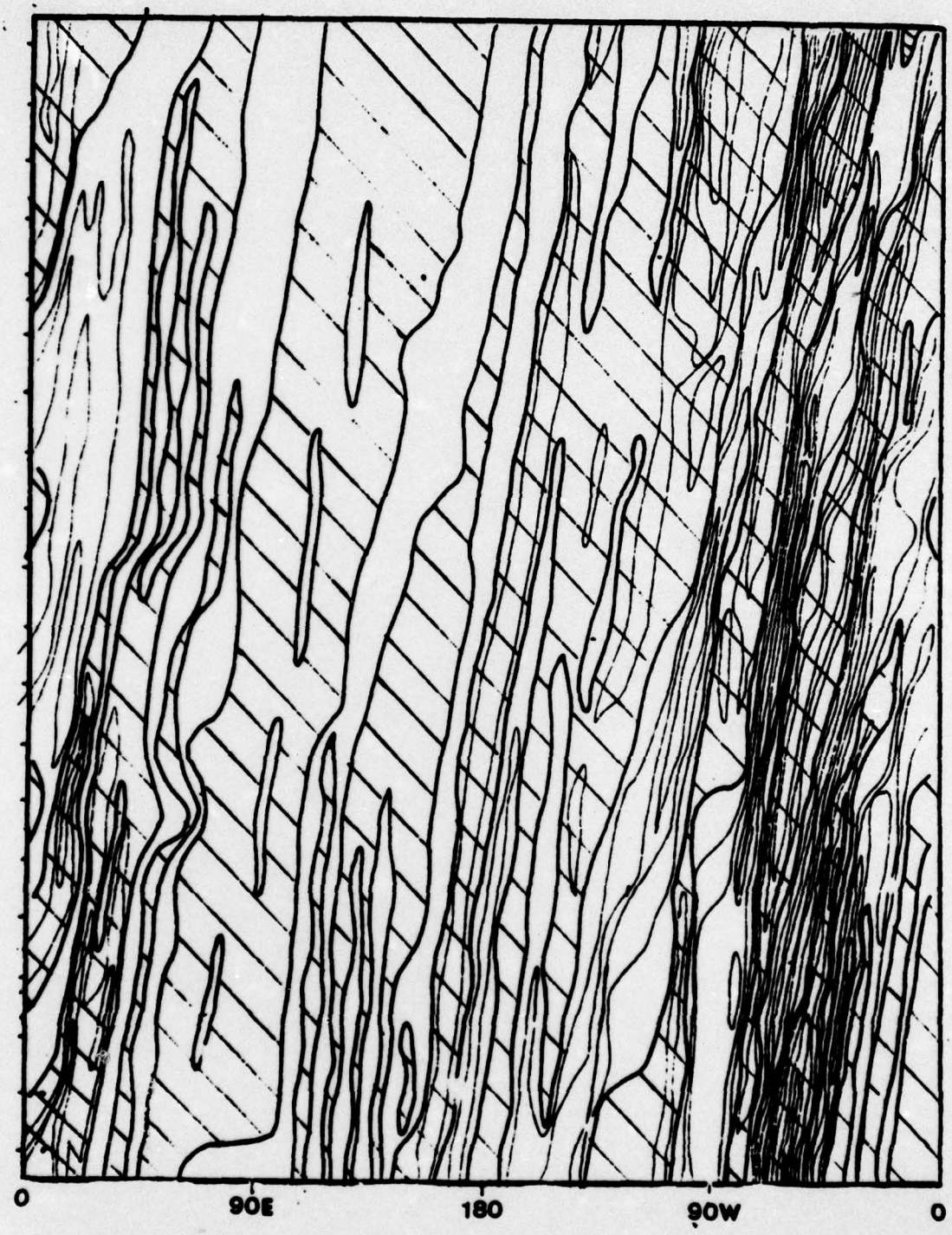

Figure 19. 250 mb vorticity time-longitude section at 12°N, fluctuating heating. Hatched area indicates positive values.

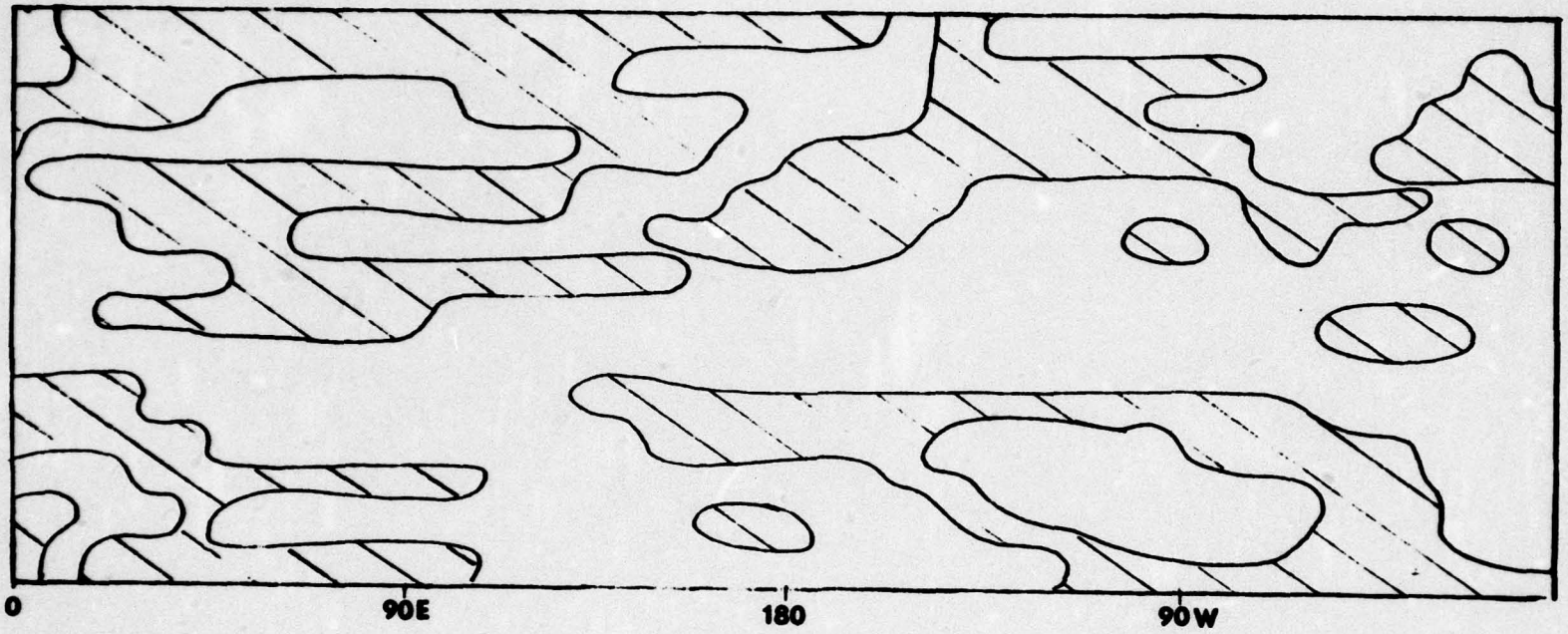

Figure 20. Meridional gradient of basic absolute vorticity fluctuating heating. Hatched area indicates positive values.

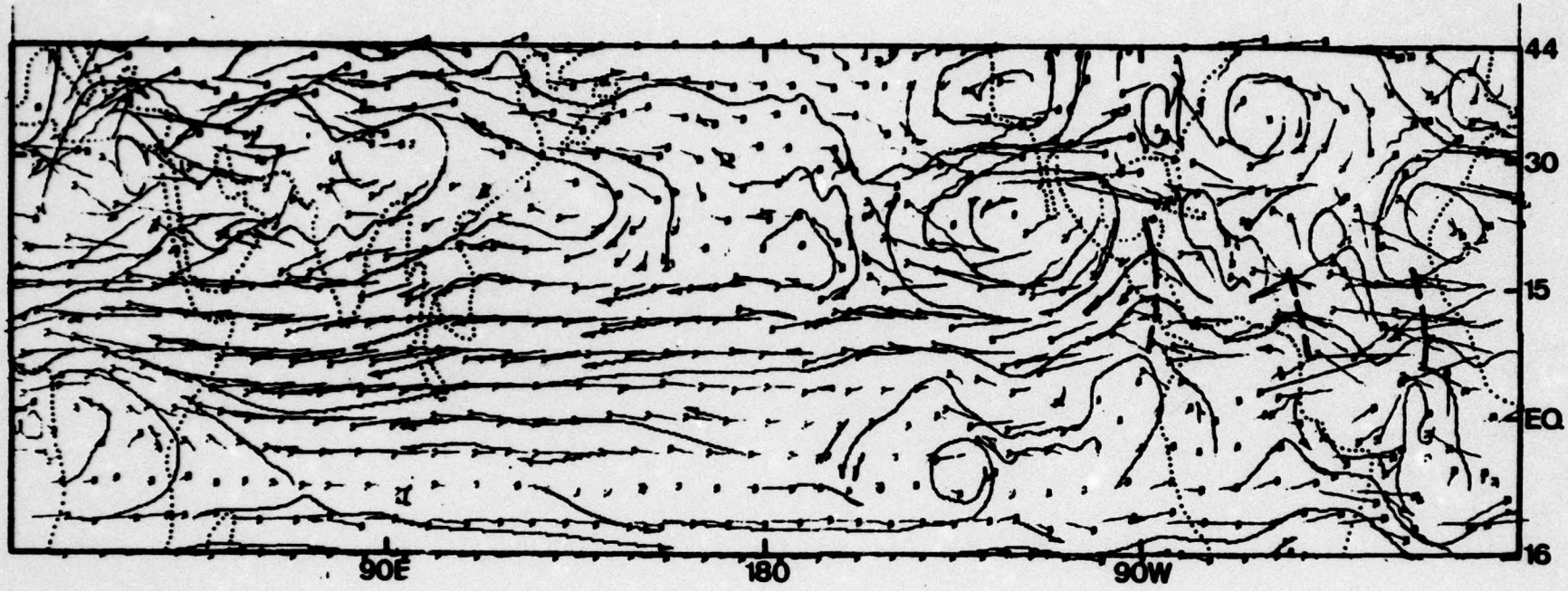

Figure 21a. 250 mb wind, fluctuating heating, Day 22.

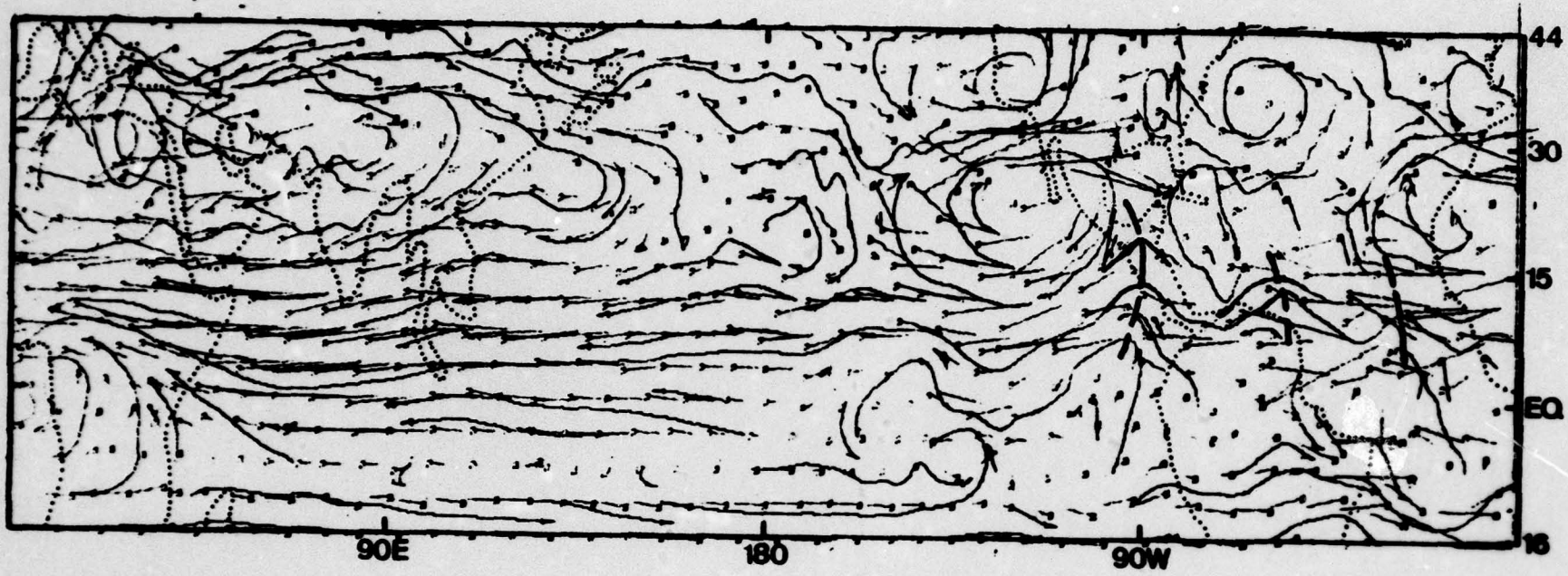

Figure 21b. 250 mb wind, fluctuating heating, Day 22.5.

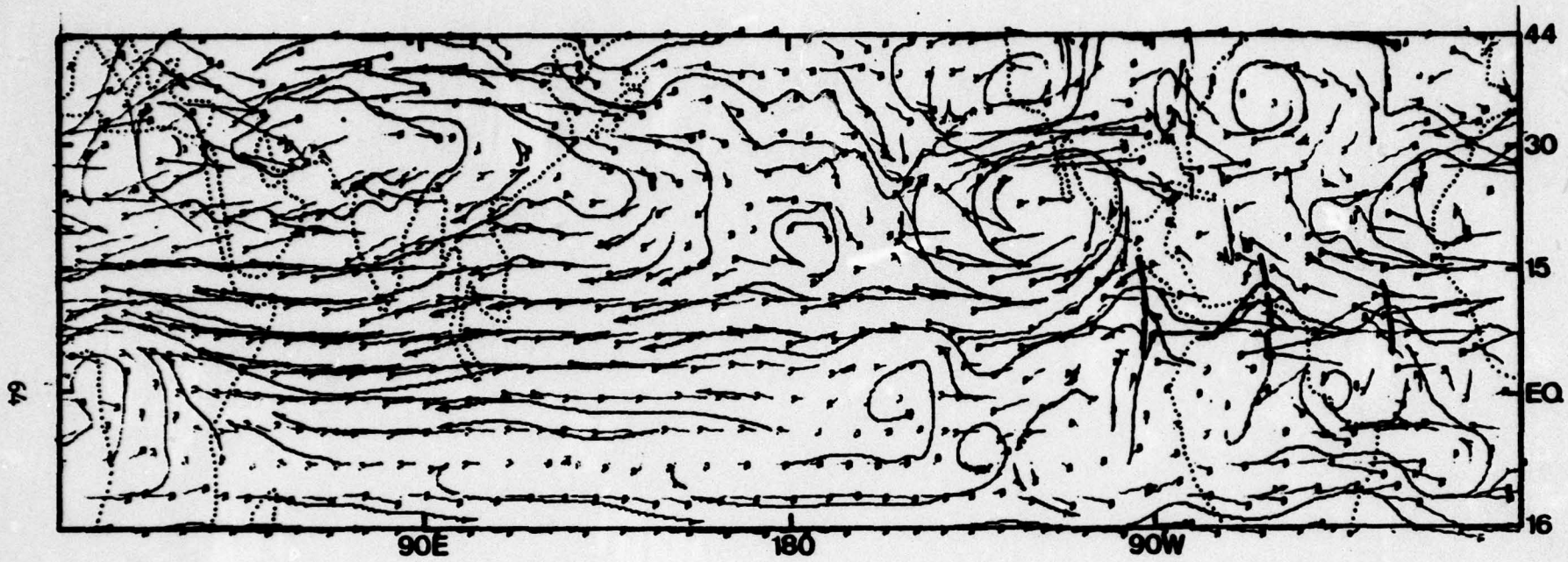

Figure 21c. 250 mb wind, fluctuating heating, Day 23.

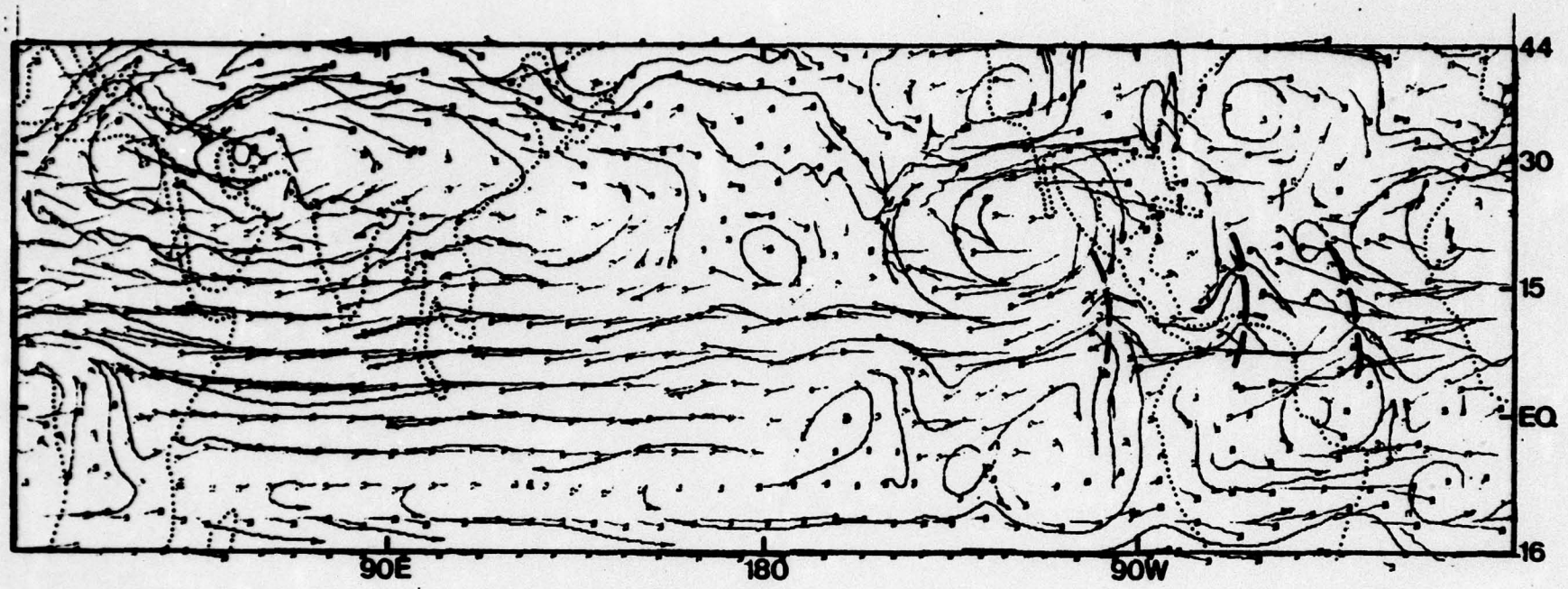

Figure 21d. 250 mb wind, fluctuating heating, Day 23.5.

LIST OF REFERENCES

1. Abbott, D. A., (1973): Scale interactions of forced quasi-stationary waves at low latitudes. Rept. 73-2, Department of Meteorology, Florida State University, Tallahassee, 190 pp.

2. Arakawa, A., and Mintz, Y., Notes of UCLA General Circulation Workshop.

3. Bellis, J. R., (1975): The modelling of monsoon circulation during northern summer, M.S. Thesis, Naval Postgraduate School, Monterey, California, 55 pp.

4. Colton, D. E., "Barotropic scale interactions in the tropical upper troposphere during the northern summer." J. Atmos. Sci., 30, 1287-1302, 1973.

5. Gates, W. L., Batten, E. S., Kahle, A. B., and Nelson, A. B., A Documentation of the Mintz-Arakawa Two-Level Atmospheric General Circulation Model, Rand, 1971.

6. Holton, J. R., and Colton, D. E., "A diagnostic study of the vorticity balance at 200 mb in the tropics during the northern summer." J. Atmos. Sci., 29, 1124-1128, 1972.

7. Krishnamurti, T. N., and Rogers, B., 200 Millibar Wind Field June, July and August, 1967, Rpt. No. 70-2, Department of Meteorology, Florida State University, Tallahassee, 1970.

8. Krishnamurti, T. N., "Observational study of the tropical upper tropospheric motion field during the Northern Hemisphere summer." J. Appl. Meteor., 10, 1066, 1096, 1971.

9. Krishnamurti, T. N., and Bhalme, H. N., "Oscillations of a monsoon system. Part I. Observational aspects." J. Atmos. Sci., 33, 1937-1954, 1976.

10. Monaco, A. V., and Williams, R. T.,(1975): An Atmospheric global prediction model using a modified Arakawa differencing scheme, M.S. Thesis, Naval Postgraduate School, Monterey, California, 86 pp.

11. Murakami, T., 1974a: "Steady and transient waves excited by diabatic heat sources during the summer monsoon." J. Atmos. Sci., 31, 340-357.

12. Sadler, J. C., The tropical upper tropospheric trough as a secondary source of typhoons and a primary source of tradewind disturbances. Final Rept., Contract AF19 (628)-3860, Air Force Cambridge Research Labs, 1967.

INITIAL DISTRIBUTION LIST

		No. Copies
1.	Defense Documentation Center Cameron Station Alexandria, Virginia 22314	2
2.	Library (Code 0142) Naval Postgraduate School Monterey, California 93940	2
3.	Assoc. Prof. C.-P. Chang, Code 63Cj Department of Meteorology Naval Postgraduate School Monterey, California 93940	6
4.	Lcdr James R. Bellis VAQ 129 NAS Whidbey Island Oak Harbor, Washington 98277	1
5.	Professor George J. Haltiner Chairman, Department of Meteorology Naval Postgraduate School Monterey, California 93940	1
6.	Department Library Department of Meteorology Naval Postgraduate School Monterey, California 93940	1
7.	Naval Oceanographic Office Library (Code 3330) Washington, D. C. 20373	1
8.	Commanding Officer Fleet Numerical Weather Central Monterey, California 93940	1
9.	Naval Environmental Prediction Research Facility Monterey, California 93940	1
10.	Dr. Roger T. Williams Department of Meteorology Naval Postgraduate School Monterey, California 93940	1
11.	Lt. Anthony V. Monaco NWSED NAF Sigonella FPO New York 09523	1

12. Director 1
Naval Oceanography and Meteorology
National Space Technology Laboratories
Bay St. Louis, Mississippi 39520

13. Lt. Richard J. Pentimonti 4
Officer in Charge
NWSED New Orleans, NAS
New Orleans, Louisiana 70146